



Optimal Error Estimates of the Local Discontinuous Galerkin Method and High-order Time Discretization Scheme for the Swift–Hohenberg Equation

Lingling Zhou¹ · Ruihan Guo²

Received: 25 May 2022 / Revised: 25 August 2022 / Accepted: 15 September 2022 /
Published online: 28 September 2022

© The Author(s), under exclusive licence to Springer Science+Business Media, LLC, part of Springer Nature 2022

Abstract

In this paper, we develop a local discontinuous Galerkin (LDG) method for the Swift–Hohenberg equation. The energy stability and optimal error estimates in L^2 norm of the semi-discrete LDG scheme are established. To avoid the severe time step restriction of explicit time marching methods, a first-order linear scheme based on the scalar auxiliary variable (SAV) method is employed for temporal discretization. Coupled with the LDG spatial discretization, we achieve a fully-discrete LDG method and prove its energy stability and optimal error estimates. To improve the temporal accuracy, the semi-implicit spectral deferred correction (SDC) method is adapted iteratively. Combining with the SAV method, the SDC method can be linear, high-order accurate and energy stable in our numerical tests. Numerical experiments are presented to verify the theoretical results and to show the efficiency of the proposed methods.

Keywords Swift–Hohenberg equation · Local discontinuous Galerkin method · Error estimate · Energy stability · Spectral deferred correction method

L. Zhou: Research supported by NSFC Grant No. 12001171.

R. Guo: Research supported by Natural Science Foundation of Henan Province, China Grant No. 222300420550.

✉ Ruihan Guo
rguo@zzu.edu.cn

Lingling Zhou
lingzhou@hpu.edu.cn

¹ School of Mathematics and Information Science, Henan Polytechnic University, Jiaozuo 454000, Henan, People's Republic of China

² School of Mathematics and Statistics, Zhengzhou University, Zhengzhou 450001, Henan, People's Republic of China

1 Introduction

The Swift–Hohenberg equation was first proposed by Swift and Hohenberg [19, 20] to model the onset and evolution of roll patterns in Rayleigh–Bénard convection. Since then, it has attracted considerable attention in several related fields, for instance, as a model for the study of pattern formation [5] and biological materials [12]. It is the gradient flow with the energy

$$E(u) = \int_{\Omega} \left(\frac{1}{2}(\Delta u + \frac{a}{2}u)^2 + \Phi(u) \right) dx, \quad (1.1)$$

where $\Omega \in \mathbb{R}^2$, $a > 0$ is a physical parameter and

$$\Phi(u) = -\frac{\varepsilon}{2}u^2 - \frac{g}{3}u^3 + \frac{u^4}{4},$$

$\varepsilon > 0$ and $g \geq 0$ are constants with physical significance.

The chemical potential is defined by the variational derivative of the energy, i.e.

$$\mu := \frac{\delta E}{\delta u} = \left(\Delta + \frac{a}{2} \right)^2 u + \Phi'(u). \quad (1.2)$$

Then the gradient flow follows

$$u_t = -\mu = -\left(\Delta + \frac{a}{2} \right)^2 u - \Phi'(u). \quad (1.3)$$

For easy presentation of the analysis, we assume a periodic boundary condition for all the variables throughout the paper. With the periodic boundary condition, the Eq. (1.3) is energy dissipative, and the dissipation rate is

$$\frac{d}{dt} E(u) = - \int_{\Omega} (u_t)^2 dx \leq 0.$$

There have been various numerical methods to simulate the Swift–Hohenberg Eq. (1.3) recently. For example, in [29], the authors presented a large time-stepping numerical method for the Swift–Hohenberg equation by adding an extra artificial term to preserve the unconditional energy stability. In [13], Lee presented first- and second-order semi-analytical Fourier spectral methods as an accurate and efficient approach for solving the Swift–Hohenberg equation based on the operator splitting method. In [14], Liu and Yin developed discontinuous Galerkin (DG) methods for spatial discretization, and the invariant energy quadratization (IEQ) method for the temporal discretization. They further proposed a multi-stage algebraically stable Runge–Kutta method and could achieve high order accuracy in both space and time in [15]. Several numerical results were presented to illustrate the efficiency of the proposed numerical schemes, but no convergence or error analyses were discussed. Qi and Hou [17] proposed and analyzed a second-order energy stable numerical scheme for the Swift–Hohenberg equation, with a mixed finite element approximation in space, and they presented an optimal error estimate for the scheme.

For spatial discretization, we will develop the high-order local discontinuous Galerkin (LDG) methods for the Swift–Hohenberg equation, since the LDG method has arbitrary high-order accuracy, easy parallelization, the flexibility for arbitrary hp adaptivity and simple treatment of boundary conditions. However, to the best knowledge of the authors, optimal error estimates of the semi-discrete and fully-discrete DG schemes for the Swift–Hohenberg equation are lacking in the existing literature. Our contribution here is that we establish the energy stability and optimal error estimates of the semi-discrete LDG scheme. The novelty

of the error analysis is that we construct the energy equality for both the primal variable and auxiliary variables to eliminate or control troublesome terms in the error equations. To estimate the nonlinear term, we show the boundness of the LDG solution with similar techniques in [10].

The LDG method considered in this paper is an extension of the DG method, which was first designed for solving linear transport equation by Reed and Hill [18] and later extended to Runge–Kutta DG (RKDG) methods for nonlinear conservation laws by Cockburn, Shu [3]. As a method developed to solve partial differential equations (PDEs) with higher-order derivatives, the LDG method was first constructed by Cockburn and Shu for convection-diffusion equations in [2]. The main idea of LDG methods is to rewrite the higher-order differential equation as a first order system by introducing auxiliary variables, then apply the traditional DG method on the system. Besides, the auxiliary variables can be locally eliminated, which is a key advantage of the scheme. Optimal error estimates of LDG methods were also obtained for the fourth order time-dependent bi-harmonic type equations [7], high order waves equations [28] and the Allen-Cahn equation [9]. For more details about LDG methods, we refer the readers to the review article [27] and the references therein.

The Swift–Hohenberg equation contains fourth-order spacial derivatives, and explicit time discretization suffers from extremely small time step restriction for stability. In this paper, we will develop a first-order linear scheme based on the scalar auxiliary variable (SAV) approach [11, 22, 23] for the Swift–Hohenberg equation. By introducing a scalar auxiliary variable to the nonlinear part of energy functional, the SAV approach has a modified energy dissipation property for a large class of gradient flows. In addition, the SAV approach leads to linear equations with constant coefficients thus it is remarkably easy to implement. Coupled with the LDG method, we will construct a fully-discrete LDG scheme and prove its energy stability and optimal convergence rate. To derive the optimal error estimates, $\mathcal{O}(h^{k+1} + \Delta t)$, we adopt a technique of the elliptic projection to deal with troublesome terms caused by auxiliary variables and jump terms of LDG schemes. In addition, we establish an extra energy equality to handle the nonlinear term of the SAV approach.

To improve the temporal accuracy, we employ the semi-implicit SDC method [8, 24] iteratively. The SDC method was first developed by Dutt et al. [6]. Then, a semi-implicit SDC method was introduced by Minion [16] to solve equations containing both stiff and nonstiff components. It is based on first-order time integration methods, which are corrected iteratively, with the order of accuracy increased by one for each additional iteration. Combining with the SAV method, the semi-implicit SDC method can be linear, high-order accurate and energy stable in our numerical tests.

The organization of the paper is as follows. In Sect. 2, we will develop the LDG method for the Swift–Hohenberg equation and prove its energy stability and optimal error estimate in L^2 norm. In Sect. 3, we first present a first-order linear temporal scheme based on the SAV approach, prove its unconditional energy stability and optimal error estimate when coupled with the LDG spatial discretization. Then, we employ the semi-implicit SDC method to achieve high-order temporal accuracy. Sect. 4 contains various numerical experiments to test the performance of the fully-discrete high-order scheme. Finally, we give concluding remarks and optimal error estimates for the elliptic projection in Sect. 5 and in the appendix, respectively.

2 Energy Stability and Error Estimate of the Semi-discrete LDG Method

In this section, we will develop the semi-discrete LDG scheme for the Swift–Hohenberg equation and establish its energy stability and error estimate.

2.1 The LDG Method and Its Energy Stability

Let $\mathcal{T}_h = \{K\}$ be a shape-regular subdivision of Ω . For example, K is a rectangle for Cartesian meshes. \mathcal{E}_h denotes the union of the boundary faces of elements $K \in \mathcal{T}_h$, and $\mathcal{E}_0 = \mathcal{E}_h \setminus \partial\Omega$. Associated with this mesh, we define the DG finite element spaces

$$V_h = \left\{ \varphi : \varphi|_K \in \mathcal{Q}^k(K), \quad \forall K \in \mathcal{T}_h \right\},$$

$$\Sigma_h = \left\{ \boldsymbol{\eta} = (\eta_1, \eta_2)^T : \eta_l|_K \in \mathcal{Q}^k(K), \quad l = 1, 2, \quad \forall K \in \mathcal{T}_h \right\},$$

where $\mathcal{Q}^k(K)$ denotes the space of tensor product of polynomials of degree at most $k \geq 0$ on $K \in \mathcal{T}_h$ in each variable. For one-dimensional case, we have $\mathcal{Q}^k(K) = \mathcal{P}^k(K)$, which is the space of polynomials of degree at most k defined on K . Set

$$(u, v)_K = \int_K uv dx, \quad (s, \boldsymbol{\theta})_K = \int_K s \cdot \boldsymbol{\theta} dx, \quad \langle u, \boldsymbol{\theta} \cdot \mathbf{n} \rangle_{\partial K} = \int_{\partial K} u \boldsymbol{\theta} \cdot \mathbf{n} ds,$$

which are the standard inner products in $L^2(K)$ and $L^2(\partial K)$, respectively. The associate L^2 norm is defined by

$$\|v\|_K^2 = (v, v)_K, \quad \|\mathbf{s}\|_K^2 = (s, s)_K, \quad \|v\|_{\partial K}^2 = \langle v, v \rangle_{\partial K}$$

and $\|v\|^2 = \sum_K \|v\|_K^2, \|\mathbf{s}\|^2 = \sum_K \|\mathbf{s}\|_K^2, \|v\|_{\mathcal{E}_h}^2 = \sum_K \|v\|_{\partial K}^2.$

To develop the LDG scheme, we first rewrite the Eq. (1.3) as a first order system

$$u_t = -\nabla \cdot \mathbf{s} - \frac{a}{2}q - p, \tag{2.1a}$$

$$\mathbf{s} = \nabla q, \tag{2.1b}$$

$$q = \nabla \cdot \boldsymbol{\omega} + \frac{a}{2}u, \tag{2.1c}$$

$$\boldsymbol{\omega} = \nabla u, \tag{2.1d}$$

$$p = \Phi'(u). \tag{2.1e}$$

The LDG scheme to solve the system (2.1) is as follows: find $u_h, q_h, p_h \in V_h$, and $s_h, \boldsymbol{\omega}_h \in \Sigma_h$, such that, for all test functions $\varphi_1, \varphi_2, \varphi_3 \in V_h$, and $\boldsymbol{\theta}_1, \boldsymbol{\theta}_2 \in \Sigma_h$, we have

$$((u_h)_t, \varphi_1)_K = (s_h, \nabla \varphi_1)_K - \langle \widehat{\mathbf{s}}_h \cdot \mathbf{n}, \varphi_1 \rangle_{\partial K} - \frac{a}{2}(q_h, \varphi_1)_K - (p_h, \varphi_1)_K, \tag{2.2a}$$

$$(s_h, \boldsymbol{\theta}_1)_K = -(q_h, \nabla \cdot \boldsymbol{\theta}_1)_K + \langle \widehat{q}_h, \boldsymbol{\theta}_1 \cdot \mathbf{n} \rangle_{\partial K}, \tag{2.2b}$$

$$(q_h, \varphi_2)_K = -(\boldsymbol{\omega}_h, \nabla \varphi_2)_K + \langle \widehat{\boldsymbol{\omega}}_h \cdot \mathbf{n}, \varphi_2 \rangle_{\partial K} + \frac{a}{2}(u_h, \varphi_2)_K, \tag{2.2c}$$

$$(\boldsymbol{\omega}_h, \boldsymbol{\theta}_2)_K = -(u_h, \nabla \cdot \boldsymbol{\theta}_2)_K + \langle \widehat{u}_h, \boldsymbol{\theta}_2 \cdot \mathbf{n} \rangle_{\partial K}, \tag{2.2d}$$

$$(p_h, \varphi_3)_K = (\Phi'(u_h), \varphi_3)_K. \tag{2.2e}$$

The ‘‘hat’’ terms in (2.2) in the cell boundary terms from integration by parts are the so-called numerical fluxes. To properly define the numerical fluxes, we need to introduce the following notations.

Let e be an interior face shared by the “left” and “right” elements K_L and K_R and define the normal vectors \mathbf{n}_L and \mathbf{n}_R on e pointing exterior to K_L and K_R , respectively. For our purpose, “left” and “right” can be uniquely defined for each face according to any fixed rule. For example, we choose \mathbf{n}_0 as a constant vector. The left element K_L to the face requires that $\mathbf{n}_L \cdot \mathbf{n}_0 < 0$, and the right one K_R requires $\mathbf{n}_R \cdot \mathbf{n}_0 \geq 0$. If ψ is a function on K_L and K_R , but possibly discontinuous across e , let ψ_L denote $(\psi|_{K_L})|_e$ and ψ_R denote $(\psi|_{K_R})|_e$, the left and right trace, respectively.

In the following proof of the energy stability and error estimate, we can see the simple alternating numerical fluxes can guarantee the energy stability, such as

$$\widehat{s}_h = (s_h)_R, \quad \widehat{q}_h = (q_h)_L, \quad \widehat{\omega}_h = (\omega_h)_R, \quad \widehat{u}_h = (u_h)_L. \tag{2.3}$$

In addition, we can see the above choice of fluxes is not unique. The crucial part is taking \widehat{s}_h and \widehat{u}_h , also $\widehat{\omega}_h$ and \widehat{q}_h from opposite sides. For the convenience of presentation, we introduce some LDG operators. Denote

$$H_K^-(r, \mathbf{v}) = (r, \nabla \cdot \mathbf{v})_K - \langle r_L, \mathbf{v} \cdot \mathbf{n} \rangle_{\partial K},$$

$$H_K^+(\mathbf{v}, r) = (\mathbf{v}, \nabla r)_K - \langle \mathbf{v}_R \cdot \mathbf{n}, r \rangle_{\partial K}.$$

Summing up over K , we define $(\cdot, \cdot) = \sum_K (\cdot, \cdot)_K$, $\langle \cdot, \cdot \rangle = \sum_K \langle \cdot, \cdot \rangle_{\partial K}$ and

$$H^-(r, \mathbf{v}) = \sum_K H_K^-(r, \mathbf{v}), \quad H^+(\mathbf{v}, r) = \sum_K H_K^+(\mathbf{v}, r).$$

With the special choice of the flux (2.3) and the periodic boundary conditions, we have the property

$$H^-(r, \mathbf{v}) = -H^+(\mathbf{v}, r). \tag{2.4}$$

Next, we will prove its energy dissipation.

Proposition 2.1 (Energy stability for the semi-discrete LDG scheme). *The solution to the LDG scheme (2.2) with the numerical fluxes (2.3) satisfies the energy stability*

$$\frac{d}{dt} \int_{\Omega} \left(\frac{1}{2} (q_h)^2 + \Phi(u_h) \right) dx \leq 0. \tag{2.5}$$

Proof First, we take the time derivative of (2.2c) and (2.2d), choose the test functions $\varphi_2 = q_h$ and $\theta_2 = -s_h$ separately to obtain

$$((q_h)_t, q_h)_K = -H_K^+((\omega_h)_t, q_h) + \frac{a}{2}((u_h)_t, q_h)_K, \tag{2.6}$$

$$-((\omega_h)_t, s_h)_K = H_K^-((u_h)_t, s_h). \tag{2.7}$$

For other equations in scheme (2.2), we choose the test functions

$$\varphi_1 = (u_h)_t, \quad \theta_1 = (\omega_h)_t, \quad \varphi_3 = -(u_h)_t,$$

respectively, to get

$$((u_h)_t, (u_h)_t)_K = H_K^+(s_h, (u_h)_t) - \frac{a}{2}(q_h, (u_h)_t)_K - (p_h, (u_h)_t)_K, \tag{2.8}$$

$$(s_h, (\omega_h)_t)_K = -H_K^-(q_h, (\omega_h)_t), \tag{2.9}$$

$$-(p_h, (u_h)_t)_K = -(\Phi'(u_h), (u_h)_t)_K. \tag{2.10}$$

Combining Eqs. (2.6)–(2.10), we find

$$\begin{aligned} & \frac{d}{dt} \int_K \left(\frac{1}{2} (q_h)^2 + \Phi(u_h) \right) dx + \int_K ((u_h)_t)^2 dx \\ & = -H_K^+((\omega_h)_t, q_h) - H_K^-(q_h, (\omega_h)_t) + H_K^-(u_h)_t, s_h) + H_K^+(s_h, (u_h)_t). \end{aligned} \tag{2.11}$$

Finally, summing up (2.11) over K and by the property (2.4), we have

$$\frac{d}{dt} \int_{\Omega} \left(\frac{1}{2} (q_h)^2 + \Phi(u_h) \right) dx + \int_{\Omega} ((u_h)_t)^2 dx = 0, \tag{2.12}$$

which implies the energy stability result (2.5). □

2.2 Error Estimate of the Semi-discrete LDG Method

In this subsection, we will present the optimal error estimate of the LDG scheme (2.2). Before stating the convergence results, we first give some projections and properties.

2.2.1 Projections and Properties

First, the one-dimensional Gauss-Radau projections $P^{\pm}u$ of a function u are defined as follows. For any $v \in P^{k-1}(K_j)$, $k \geq 1$, and an arbitrary subinterval $K_j = (x_{j-1}, x_j)$, there hold

$$(P^-u, v)_{K_j} = (u, v)_{K_j}, \quad P^-u(x_j) = u(x_j), \tag{2.13}$$

$$(P^+u, v)_{K_j} = (u, v)_{K_j}, \quad P^+u(x_{j-1}) = u(x_{j-1}). \tag{2.14}$$

For Cartesian meshes in two dimension, we define the projection P^- for scalar functions on a two-dimensional rectangle element $I \otimes J = [x_{i-1}, x_i] \times [y_{j-1}, y_j]$ as

$$P^- = P_x^- \otimes P_y^-, \tag{2.15}$$

where the subscripts x and y indicate the one-dimensional projections defined by (2.13).

Denote the standard L^2 projection in x and y direction by π_x, π_y , respectively. The projection Π^+ for a vector-valued function $\theta = (\theta_1(x, y), \theta_2(x, y))$ is defined by

$$\Pi^+ : [H^1(\Omega)]^2 \longrightarrow [\mathcal{Q}^k(I \otimes J)]^2, \quad \theta \longmapsto \Pi^+\theta = (P_x^+ \otimes \pi_y \theta_1, \pi_x \otimes P_y^+ \theta_2), \tag{2.16}$$

where P_x^+ and P_y^+ are the one-dimensional projections defined in (2.14). Note that the projection $\Pi^+\theta$ satisfies the following properties, for any $\varphi \in \mathcal{Q}^k(I \otimes J)$,

$$\int_I \int_J (\Pi^+\theta - \theta) \cdot \nabla \varphi dy dx = 0, \tag{2.17a}$$

$$\int_J (\Pi^+\theta(x_{i-1}, y) - \theta(x_{i-1}, y)) \cdot \mathbf{n} \varphi(x_{i-1}^+, y) dy = 0, \tag{2.17b}$$

$$\int_I (\Pi^+\theta(x, y_{j-1}) - \theta(x, y_{j-1})) \cdot \mathbf{n} \varphi(x, y_{j-1}^+) dx = 0. \tag{2.17c}$$

In addition, we have the following approximation properties of the projections mentioned above,

$$\|P^-u - u\|_{H^m(\mathcal{T}_h)} + h^{1/2-m} \|P^-u - u\|_{\mathcal{E}_h} \leq Ch^{\min\{r, k+1\}-m} \|u\|_{H^r(\Omega)}, \tag{2.18a}$$

$$\|\Pi^+\theta - \theta\|_{H^m(\mathcal{T}_h)} + h^{1/2-m} \|(\Pi^+\theta - \theta) \cdot \mathbf{n}\|_{\mathcal{E}_h} \leq Ch^{\min\{r, k+1\}-m} \|\theta\|_{H^r(\Omega)}, \tag{2.18b}$$

for $0 \leq m \leq \min\{r, k + 1\}$. Here the positive constant C is independent of h . The projection P^- on the Cartesian meshes defined by (2.15) has the following superconvergence property (see [4], Lemma 3.6). For more details about the projections, we refer readers to [1, 7].

Lemma 2.2 *Suppose $(u, \theta) \in H^{k+2}(\Omega) \otimes \Sigma_h$, then the projection P^- defined by (2.15) satisfies*

$$|(u - P^-u, \nabla \cdot \theta) - (u - \widehat{P^-u}, \theta \cdot n)| \leq Ch^{k+1} \|u\|_{H^{k+2}(\Omega)} \|\theta\|, \tag{2.19}$$

where the ‘‘hat’’ term is the numerical flux.

2.2.2 Error Equations

Denote

$$e_r = r - r_h, \quad e_z = z - z_h$$

for $r = u, q, p$ and $z = s, \omega$. Let P and Π be the projections defined in the above subsection. By adding and subtracting projections Pr and Πz , we divide the error into

$$e_r = r - Pr + Pr - r_h = \eta_r + \zeta_r, \quad e_z = z - \Pi z + \Pi z - z_h = \eta_z + \zeta_z.$$

Here we take the projections $(P, \Pi) = (P^-, P^+)$ defined by (2.13)–(2.14) for the one-dimensional space, and take $(P, \Pi) = (P^-, \Pi^+)$ defined by (2.15)–(2.16) for two-dimensional Cartesian meshes. Note that the exact solutions u, q, p, s, ω of the problem (2.1) also satisfy (2.2). We obtain the error equations

$$((\zeta_u)_t, \varphi_1)_K = H_K^+(\zeta_s, \varphi_1) - \frac{a}{2}(e_q, \varphi_1)_K - (e_p, \varphi_1)_K - ((\eta_u)_t, \varphi_1)_K, \tag{2.20a}$$

$$(\zeta_s, \theta_1)_K = -H_K^-(\zeta_q, \theta_1) - (\eta_s, \theta_1)_K - H_K^-(\eta_q, \theta_1), \tag{2.20b}$$

$$(\zeta_q, \varphi_2)_K = -H_K^+(\zeta_\omega, \varphi_2) + \frac{a}{2}(e_u, \varphi_2)_K - (\eta_q, \varphi_2)_K, \tag{2.20c}$$

$$(\zeta_\omega, \theta_2)_K = -H_K^-(\zeta_u, \theta_2) - (\eta_\omega, \theta_2)_K - H_K^-(\eta_u, \theta_2), \tag{2.20d}$$

$$(e_p, \varphi_3)_K = (\Phi'(u) - \Phi'(u_h), \varphi_3)_K \tag{2.20e}$$

for any $\varphi_1, \varphi_2, \varphi_3 \in V_h$, and $\theta_1, \theta_2 \in \Sigma_h$. Here we use the property (2.17) of the projections, i.e., $H_K^+(\eta_s, \varphi_1) = 0$ and $H_K^+(\eta_\omega, \varphi_2) = 0$.

2.2.3 Optimal Error Estimates in L^2 Norm

To deal with the nonlinear term in the analysis, we show the estimate for the numerical solution u_h . Along the same idea as that in [10], the following lemma is required and thus we need to introduce the ‘‘discrete Laplacian’’ operator [21] firstly.

For the second-order elliptic problem with a periodic boundary condition

$$-\Delta u = f, \tag{2.21}$$

where f is a given function, the LDG discrete Laplacian operator can be derived through its first order version

$$\begin{aligned} \nabla u &= z, \\ -\nabla \cdot z &= f. \end{aligned}$$

Multiplying the first and second equations by the test functions θ and ϑ , respectively, and integrating on K , we define the LDG “discrete Laplacian” Δ_h as follows: given $u_h \in V_h$, find $-\Delta_h u_h \in V_h$ such that

$$(z_h, \theta)_K = -(u_h, \nabla \cdot \theta)_K + \langle \hat{u}_h, \theta \cdot \mathbf{n} \rangle_{\partial K}, \tag{2.22}$$

$$(-\Delta_h u_h, \vartheta)_K = (z_h, \nabla \vartheta)_K - \langle \hat{z}_h \cdot \mathbf{n}, \vartheta \rangle_{\partial K}, \tag{2.23}$$

where $\hat{u}_h = (u_h)_L, \hat{z}_h = (z_h)_R$. The well-posedness of the operator can be obtained in $V_h^0 := \{v \in V_h : (v, 1) = 0\}$.

Lemma 2.3 [21] *For any $u_h \in V_h^0$, we have*

$$\|u_h\|_\infty \leq C(1 + \|z_h\|)\sqrt{\log(1 + \|\Delta_h u_h\|)},$$

where z_h satisfies (2.22).

Next we can obtain the estimate for the numerical solution.

Lemma 2.4 *The solution of the LDG scheme (2.2) satisfies*

$$\|u_h\| \leq C, \quad \|q_h\| \leq C, \quad \|\omega_h\| \leq C, \quad \|u_h\|_\infty \leq C,$$

where $C > 0$ is independent of h .

Proof Applying Cauchy’s inequality, we have

$$\frac{d}{dt}(u_h, u_h) = 2(u_h, (u_h)_t) \leq 2(u_h, u_h) + \frac{1}{2}((u_h)_t, (u_h)_t).$$

Thus the energy equality (2.12) turns out to be

$$\frac{d}{dt} \int_\Omega \left(\frac{1}{2}(q_h)^2 + (u_h)^2 + \Phi(u_h) \right) dx + \frac{1}{2} \int_\Omega ((u_h)_t)^2 dx \leq 2(u_h, u_h).$$

By Gronwall’s inequality, we derive

$$\begin{aligned} & \left(\frac{1}{2}(q_h, q_h) + (u_h, u_h) + (\Phi(u_h), 1) \right) (t) \\ & \leq e^{2t} \left(\frac{1}{2}(q_h, q_h) + (u_h, u_h) + (\Phi(u_h), 1) \right) (0) \leq C. \end{aligned}$$

where the last inequality holds because of the choice of the initial condition. By Young’s inequality, we have

$$\int_\Omega u_h^3 dx \leq \int_\Omega \left(\frac{\delta}{2} u_h^4 + \frac{1}{2\delta} u_h^2 \right) dx,$$

which implies

$$\int_\Omega \Phi(u_h) dx \geq \left(\frac{1}{4} - \frac{g\delta}{6} \right) \int_\Omega u_h^4 dx - \left(\frac{g}{6\delta} + \frac{\varepsilon}{2} \right) \int_\Omega u_h^2 dx.$$

Thus

$$\frac{1}{2}(q_h, q_h) + (u_h, u_h) + (\Phi(u_h), 1) \geq \int_\Omega \left(\frac{1}{2} q_h^2 + \left(1 - \frac{g}{6\delta} - \frac{\varepsilon}{2} \right) u_h^2 + \left(\frac{1}{4} - \frac{g\delta}{6} \right) u_h^4 \right) dx.$$

Choose δ such that

$$1 - \frac{g}{6\delta} - \frac{\varepsilon}{2} > 0, \quad \frac{1}{4} - \frac{g\delta}{6} \geq 0,$$

which yields

$$\|u_h\| \leq C, \quad \|q_h\| \leq C.$$

Taking the test functions $\varphi_2 = u_h, \theta_2 = \omega_h$ in (2.2c)–(2.2d) derives

$$\begin{aligned} (q_h, u_h)_K &= -(\omega_h, \nabla u_h)_K + \langle \widehat{\omega}_h \cdot \mathbf{n}, u_h \rangle_{\partial K} + \frac{a}{2}(u_h, u_h)_K, \\ (\omega_h, \omega_h)_K &= -(u_h, \nabla \cdot \omega_h)_K + \langle \widehat{u}_h, \omega_h \cdot \mathbf{n} \rangle_{\partial K}. \end{aligned}$$

Adding them together and summing up over K , we get

$$\|\omega_h\|^2 = \frac{a}{2}(u_h, u_h) - (q_h, u_h) \leq \frac{a+1}{2}\|u_h\|^2 + \frac{1}{2}\|q_h\|^2 \leq C.$$

Note that the “discrete Laplacian” operator $\Delta_h u_h$ is defined by

$$\begin{aligned} (\Delta_h u_h, v)_K &= -(\omega_h, \nabla v)_K + \langle \widehat{\omega}_h \cdot \mathbf{n}, v \rangle_{\partial K} \\ &= (q_h, v)_K - \frac{a}{2}(u_h, v)_K, \quad v \in V_h, \end{aligned}$$

where the second equality is by (2.2c). Taking $v = \Delta_h u_h$ in the above equation leads to

$$\|\Delta_h u_h\| \leq \frac{a}{2}\|u_h\| + \|q_h\| \leq C.$$

Applying Lemma 2.3, we obtain

$$\|u_h\|_\infty \leq C(1 + \|\omega_h\|)\sqrt{\log(1 + \|\Delta_h u_h\|)} \leq C,$$

which completes the proof. □

We would like to assume the exact solution of Eq. (1.3) has the following smoothness:

$$u \in L^\infty(0, T; H^{k+4}), \quad u_t \in L^\infty(0, T; H^{k+3}). \tag{2.24}$$

Now we are ready to derive the optimal error estimate of the semi-discrete LDG scheme (2.2).

Theorem 2.5 *Let u_h be the numerical solution of the scheme (2.2), and u be the exact solution of equation (1.3). Suppose u satisfies the smoothness assumption (2.24), then there exists a constant C , such that*

$$\|u(\cdot, T) - u_h(\cdot, T)\| \leq Ch^{k+1}, \tag{2.25}$$

where C is independent of h, u_h and dependent on $k, T, \|u\|_{L^\infty(0,T;H^{k+4}(\Omega))}$ and $\|u_t\|_{L^\infty(0,T;H^{k+3}(\Omega))}$.

Proof Taking the test functions $\varphi_1 = \zeta_u, \theta_1 = \zeta_\omega, \varphi_2 = \zeta_q, \theta_2 = -\zeta_s, \varphi_3 = -\zeta_u$ in the error Eq. (2.20), respectively, and adding them together, we have

$$((\zeta_u)_t, \zeta_u)_K + (\zeta_q, \zeta_q)_K = RHS,$$

where

$$\begin{aligned}
 RHS = & -((\eta_u)_t, \zeta_u)_K - (\eta_s, \zeta_\omega)_K - (\eta_q, \zeta_q)_K + (\eta_\omega, \zeta_s)_K - \frac{a}{2}(\eta_q, \zeta_u)_K + \frac{a}{2}(\eta_u, \zeta_q)_K \\
 & + H_K^+(\zeta_s, \zeta_u) + H_K^-(\zeta_u, \zeta_s) - H_K^-(\zeta_q, \zeta_\omega) - H_K^+(\zeta_\omega, \zeta_q) \\
 & - H_K^-(\eta_q, \zeta_\omega) + H_K^-(\eta_u, \zeta_s) - (\Phi'(u) - \Phi'(u_h), \zeta_u)_K.
 \end{aligned}$$

Summing up over K and by the property (2.4), we obtain the first energy equality in the form of ζ_u and ζ_q ,

$$((\zeta_u)_t, \zeta_u) + (\zeta_q, \zeta_q) = S_1, \tag{2.26}$$

where

$$\begin{aligned}
 S_1 = & -((\eta_u)_t, \zeta_u) - (\eta_s, \zeta_\omega) - (\eta_q, \zeta_q) + (\eta_\omega, \zeta_s) - \frac{a}{2}(\eta_q, \zeta_u) + \frac{a}{2}(\eta_u, \zeta_q) \\
 & - H^-(\eta_q, \zeta_\omega) + H^-(\eta_u, \zeta_s) - (\Phi'(u) - \Phi'(u_h), \zeta_u).
 \end{aligned}$$

Taking the time derivative of (2.20d), we have

$$((\zeta_\omega)_t, \theta_2)_K = -H_K^-(\zeta_u)_t, \theta_2) - ((\eta_\omega)_t, \theta_2) - H_K^-(\eta_u)_t, \theta_2). \tag{2.27}$$

Choosing test functions $\varphi_1 = -\zeta_q, \theta_1 = \zeta_s, \varphi_2 = (\zeta_u)_t$ in the error Eqs. (2.20a)–(2.20c), $\theta_2 = \zeta_\omega$ in (2.27), and $\varphi_3 = \zeta_q$ in (2.20e), we derive

$$\begin{aligned}
 ((\zeta_u)_t, -\zeta_q)_K &= H_K^+(\zeta_s, -\zeta_q) - \frac{a}{2}(e_q, -\zeta_q)_K - (e_p, -\zeta_q)_K - ((\eta_u)_t, -\zeta_q)_K, \\
 (\zeta_s, \zeta_s)_K &= -H_K^-(\zeta_q, \zeta_s) - (\eta_s, \zeta_s)_K - H_K^-(\eta_q, \zeta_s), \\
 (\zeta_q, (\zeta_u)_t)_K &= -H_K^+(\zeta_\omega, (\zeta_u)_t) + \frac{a}{2}(e_u, (\zeta_u)_t)_K - (\eta_q, (\zeta_u)_t)_K, \\
 ((\zeta_\omega)_t, \zeta_\omega)_K &= -H_K^-(\zeta_u)_t, \zeta_\omega) - ((\eta_\omega)_t, \zeta_\omega)_K - H_K^-(\eta_u)_t, \zeta_\omega), \\
 (e_p, \zeta_q)_K &= (\Phi'(u) - \Phi'(u_h), \zeta_q)_K.
 \end{aligned}$$

Adding them together, summing up over K and by the property (2.4), we obtain the second energy equality in the form of ζ_s and ζ_ω ,

$$((\zeta_\omega)_t, \zeta_\omega) + (\zeta_s, \zeta_s) - \frac{a}{2}(\zeta_q, \zeta_q) - \frac{a}{2}(\zeta_u, (\zeta_u)_t) = S_2, \tag{2.28}$$

where

$$\begin{aligned}
 S_2 = & ((\eta_u)_t, \zeta_q) - (\eta_s, \zeta_s) - (\eta_q, (\zeta_u)_t) - ((\eta_\omega)_t, \zeta_\omega) + \frac{a}{2}(\eta_q, \zeta_q) + \frac{a}{2}(\eta_u, (\zeta_u)_t) \\
 & - H^-(\eta_q, \zeta_s) - H^-(\eta_u)_t, \zeta_\omega) + (\Phi'(u) - \Phi'(u_h), \zeta_q).
 \end{aligned}$$

Then, $a \times (2.26) + (2.28)$ gives

$$\frac{a}{2}((\zeta_u)_t, \zeta_u) + \frac{a}{2}(\zeta_q, \zeta_q) + ((\zeta_\omega)_t, \zeta_\omega) + (\zeta_s, \zeta_s) = T_1 + T_2 + T_3 + T_4, \tag{2.29}$$

where

$$\begin{aligned}
 T_1 = & -a((\eta_u)_t, \zeta_u) - a(\eta_s, \zeta_\omega) - a(\eta_q, \zeta_q) + a(\eta_\omega, \zeta_s) - \frac{a^2}{2}(\eta_q, \zeta_u) + \frac{a^2}{2}(\eta_u, \zeta_q) \\
 & + ((\eta_u)_t, \zeta_q) - (\eta_s, \zeta_s) - ((\eta_\omega)_t, \zeta_\omega) + \frac{a}{2}(\eta_q, \zeta_q), \\
 T_2 = & -(\eta_q, (\zeta_u)_t) + \frac{a}{2}(\eta_u, (\zeta_u)_t),
 \end{aligned}$$

$$\begin{aligned}
 T_3 &= -aH^-(\eta_q, \zeta_\omega) + aH^-(\eta_u, \zeta_s) - H^-(\eta_q, \zeta_s) - H^-((\eta_u)_t, \zeta_\omega). \\
 T_4 &= -a(\Phi'(u) - \Phi'(u_h), \zeta_u) + (\Phi'(u) - \Phi'(u_h), \zeta_q).
 \end{aligned}$$

By Cauchy–Schwarz inequality, the approximation properties (2.18) and the linearity of the projections, we get

$$T_1 \leq Ch^{k+1}(\|\zeta_u\| + \|\zeta_q\| + \|\zeta_s\| + \|\zeta_\omega\|).$$

As for the term T_3 , Lemma 2.2 implies that

$$T_3 \leq Ch^{k+1}(\|\zeta_s\| + \|\zeta_\omega\|).$$

Considering the nonlinear term T_4 , we apply Lagrange’s mean value theorem to obtain

$$\begin{aligned}
 T_4 &= -a(\Phi''(\xi)(u - u_h), \zeta_u) + (\Phi''(\xi)(u - u_h), \zeta_q) \\
 &\leq C\left(|(u - u_h, \zeta_u)| + |(u - u_h, \zeta_q)|\right),
 \end{aligned}$$

where ξ is between u and u_h . Here we use the fact that $\|u_h\|_\infty \leq C$ derived in Lemma 2.4 and $\Phi(u)$ is a polynomial of u . Note that $u - u_h = \zeta_u + \eta_u$. The estimate of T_4 turns out to be

$$\begin{aligned}
 T_4 &\leq C(\|\eta_u\| \|\zeta_u\| + \|\zeta_u\|^2 + \|\eta_u\| \|\zeta_q\| + \|\zeta_u\| \|\zeta_q\|) \\
 &\leq C\|\zeta_u\|^2 + \frac{a}{4}\|\zeta_q\|^2 + Ch^{2k+2}.
 \end{aligned}$$

Here the approximation properties (2.18) are used again. Combine the estimates of T_1, T_3, T_4 and the energy equality (2.29) together to get

$$\begin{aligned}
 &\frac{d}{dt} \left(\frac{a}{4}\|\zeta_u\|^2 + \frac{1}{2}\|\zeta_\omega\|^2 \right) + \frac{a}{2}\|\zeta_q\|^2 + \|\zeta_s\|^2 \\
 &\leq C\|\zeta_u\|^2 + \frac{1}{4}\|\zeta_\omega\|^2 + \frac{a}{2}\|\zeta_q\|^2 + \|\zeta_s\|^2 + Ch^{2k+2} + T_2.
 \end{aligned} \tag{2.30}$$

For the term T_2 , using integration by parts with respect to t , we have

$$\begin{aligned}
 \int_0^T T_2 dt &= \int_0^T \left[\frac{a}{2}(\eta_u, (\zeta_u)_t) - (\eta_q, (\zeta_u)_t) \right] dt \\
 &= \left(\frac{a}{2}(\eta_u, \zeta_u) - (\eta_q, \zeta_u) \right) \Big|_0^T - \int_0^T \left[\frac{a}{2}((\eta_u)_t, \zeta_u) - ((\eta_q)_t, \zeta_u) \right] dt \\
 &\leq \frac{a}{8}\|\zeta_u(T)\|^2 + \frac{a}{8}\|\zeta_u(0)\|^2 + \int_0^T \|\zeta_u\|^2 dt + Ch^{2k+2}.
 \end{aligned}$$

Integrating (2.30) with respect to t to obtain

$$\begin{aligned}
 &\frac{a}{4}\|\zeta_u(T)\|^2 + \frac{1}{2}\|\zeta_\omega(T)\|^2 \\
 &\leq \int_0^T \left(C\|\zeta_u\|^2 + \frac{1}{4}\|\zeta_\omega\|^2 + T_2 \right) dt + \frac{a}{4}\|\zeta_u(0)\|^2 + \frac{1}{2}\|\zeta_\omega(0)\|^2 + Ch^{2k+2}.
 \end{aligned}$$

With the special choice of the initial condition, it is easy to see that

$$\|\zeta_u(0)\| \leq Ch^{k+1}, \quad \|\zeta_\omega(0)\| \leq Ch^{k+1}.$$

Thus

$$\frac{a}{8} \|\zeta_u(T)\|^2 + \frac{1}{2} \|\zeta_\omega(T)\|^2 \leq \int_0^T \left(C \|\zeta_u\|^2 + \frac{1}{4} \|\zeta_\omega\|^2 \right) dt + Ch^{2k+2}.$$

Finally, the optimal error estimate (2.25) follows by using Gronwall’s inequality and triangle inequality. \square

3 Time Discretization

In this section, we first describe a first-order time stepping scheme for the Swift–Hohenberg equation, which is based on the SAV approach. Coupled with the LDG spatial discretization, we then achieve the fully-discrete LDG scheme and prove its energy stability and optimal error estimates. Lastly, we employ the semi-implicit SDC method iteratively to improve the temporal accuracy.

3.1 A Linear Scheme in Time

In order to develop a linear and energy stable scheme, we first describe the SAV approach [23] briefly. Let $E_1(u) = \int_\Omega \Phi(u)dx$. Then we introduce the scalar variable $r(t) = \sqrt{E_1(u) + B}$, where B is a constant to ensure $E_1(u) + B \geq 0$.

Using the variable r , the energy functional (1.1) can be recast as

$$E(u, r) = \int_\Omega \left(\frac{1}{2} (\Delta u + \frac{a}{2} u)^2 \right) dx + r^2 - B. \tag{3.1}$$

Then, we have the following equivalent equation

$$u_t = - \left(\Delta + \frac{a}{2} \right)^2 u - \frac{r}{\sqrt{E_1(u) + B}} \Phi'(u), \tag{3.2}$$

$$r_t = \frac{1}{2\sqrt{E_1(u) + B}} \int_\Omega \Phi'(u) u_t dx. \tag{3.3}$$

The initial conditions are

$$u(t = 0) = u_0, \quad r(t = 0) = \sqrt{E_1(u_0) + B}.$$

Further, the equivalent equation preserves an energy law, i.e.

$$\frac{d}{dt} E(u, r) = - \int_\Omega (u_t)^2 dx \leq 0. \tag{3.4}$$

Obviously, we hope to construct a linear scheme that preserve the energy law (3.4) in the discrete sense. A first-order SAV scheme can be given as follows

$$\frac{u^{n+1} - u^n}{\Delta t} = - \left(\Delta + \frac{a}{2} \right)^2 u^{n+1} - \frac{r^{n+1}}{\sqrt{E_1(u^n) + B}} \Phi'(u^n), \tag{3.5}$$

$$\frac{r^{n+1} - r^n}{\Delta t} = \frac{1}{2\sqrt{E_1(u^n) + B}} \int_\Omega \Phi'(u^n) \frac{u^{n+1} - u^n}{\Delta t} dx. \tag{3.6}$$

Since (3.6) is a simple algebraic equation, we can rewrite it as

$$r^{n+1} = r^n + \frac{1}{2\sqrt{E_1(u^n) + B}} \int_\Omega \Phi'(u^n) (u^{n+1} - u^n) dx.$$

Denote

$$b^n = \Phi'(u^n)/\sqrt{E_1(u^n) + B}.$$

Then the scheme (3.5) can be written as

$$\frac{u^{n+1} - u^n}{\Delta t} = -\left(\Delta + \frac{a}{2}\right)^2 u^{n+1} - b^n \left(r^n + \frac{1}{2} \int_{\Omega} b^n(u^{n+1} - u^n) dx\right). \tag{3.7}$$

Now, we show an efficient implementation of the scheme (3.5). We derive from (3.7) that

$$\left(I + \Delta t \left(\Delta + \frac{a}{2}\right)^2\right) u^{n+1} + \frac{\Delta t}{2} b^n(b^n, u^{n+1}) = u^n - \Delta t b^n r^n + \frac{\Delta t}{2} b^n(b^n, u^n). \tag{3.8}$$

Denote the right hand side of (3.8) by c^n . Multiplying (3.8) with $(I + \Delta t(\Delta + \frac{a}{2})^2)^{-1}$, then taking the inner product with b^n , we obtain

$$(b^n, u^{n+1}) + \frac{\Delta t}{2} \gamma^n(b^n, u^{n+1}) = \left(b^n, \left(I + \Delta t \left(\Delta + \frac{a}{2}\right)^2\right)^{-1} c^n\right), \tag{3.9}$$

where $\gamma^n = (b^n, (I + \Delta t(\Delta + \frac{a}{2})^2)^{-1} b^n)$. Hence

$$(b^n, u^{n+1}) = \frac{(b^n, (I + \Delta t(\Delta + \frac{a}{2})^2)^{-1} c^n)}{1 + \Delta t \gamma^n / 2}. \tag{3.10}$$

The details related to the scheme implementation are summarized in the following algorithm.

- Step 1** Compute b^n and c^n ;
- Step 2** Compute (b^n, u^{n+1}) by (3.10);
- Step 3** Compute u^{n+1} by (3.8) and r^{n+1} by (3.6), then goto the next step.

3.2 The Fully-Discrete LDG Scheme and Its Energy Stability

In this subsection, we will develop the LDG scheme to solve the linear scheme (3.5)–(3.6). Firstly we rewrite it as a first order system

$$\frac{u^{n+1} - u^n}{\Delta t} = -\nabla \cdot s^{n+1} - \frac{a}{2} q^{n+1} - r^{n+1} b^n, \tag{3.11a}$$

$$s^{n+1} = \nabla q^{n+1}, \tag{3.11b}$$

$$q^{n+1} = \nabla \cdot \omega^{n+1} + \frac{a}{2} u^{n+1}, \tag{3.11c}$$

$$\omega^{n+1} = \nabla u^{n+1}. \tag{3.11d}$$

The LDG scheme to solve the linear scheme (3.5)–(3.6) becomes the following: find $u_h^{n+1}, q_h^{n+1} \in V_h$ and $s_h^{n+1}, \omega_h^{n+1} \in \Sigma_h$ such that, for all test functions $\varphi_1, \varphi_2 \in V_h$ and $\theta_1, \theta_2 \in \Sigma_h$, we have

$$\frac{1}{\Delta t} (u_h^{n+1} - u_h^n, \varphi_1)_K = H_K^+(s_h^{n+1}, \varphi_1) - \frac{a}{2} (q_h^{n+1}, \varphi_1)_K - (r_h^{n+1} b_h^n, \varphi_1)_K, \tag{3.12a}$$

$$(s_h^{n+1}, \theta_1)_K = -H_K^-(q_h^{n+1}, \theta_1), \tag{3.12b}$$

$$(q_h^{n+1}, \varphi_2)_K = -H_K^+(\omega_h^{n+1}, \varphi_2) + \frac{a}{2}(u_h^{n+1}, \varphi_2)_K, \tag{3.12c}$$

$$(\omega_h^{n+1}, \theta_2)_K = -H_K^-(u_h^{n+1}, \theta_2), \tag{3.12d}$$

where

$$r_h^{n+1} = r_h^n + \frac{1}{2\sqrt{E_1(u_h^n) + B}} \int_{\Omega} \Phi'(u_h^n)(u_h^{n+1} - u_h^n) dx, \tag{3.13}$$

$$b_h^n = \Phi'(u_h^n) / \sqrt{E_1(u_h^n) + B}.$$

The numerical fluxes are

$$\widehat{s}_h^{n+1} = (s_h^{n+1})_R, \quad \widehat{q}_h^{n+1} = (q_h^{n+1})_L, \quad \widehat{\omega}_h^{n+1} = (\omega_h^{n+1})_R, \quad \widehat{u}_h^{n+1} = (u_h^{n+1})_L. \tag{3.14}$$

Next, we will prove its energy dissipation.

Proposition 3.1 (Energy stability for the fully-discrete LDG scheme). *The solution to the LDG scheme (3.12) with the numerical fluxes (3.14) satisfies the energy stability*

$$E_h(q_h^{n+1}, r_h^{n+1}) + \frac{1}{\Delta t} \int_{\Omega} (u_h^{n+1} - u_h^n)^2 dx \leq E_h(q_h^n, r_h^n), \tag{3.15}$$

where

$$E_h(q_h, r_h) = \frac{1}{2} \int_{\Omega} q_h^2 dx + r_h^2.$$

Proof Let $\mathcal{D}u$ denote $u_h^{n+1} - u_h^n$. For (3.12c) and (3.12d), subtracting the equations at time level t^n from the equations at time level t^{n+1} , choosing the test function $\varphi_2 = q_h^{n+1}$ and $\theta_2 = -s_h^{n+1}$, we obtain

$$(\mathcal{D}q, q_h^{n+1})_K = -H_K^+(\mathcal{D}\omega, q_h^{n+1}) + \frac{a}{2}(\mathcal{D}u, q_h^{n+1})_K, \tag{3.16}$$

$$-(\mathcal{D}\omega, s_h^{n+1})_K = H_K^-(\mathcal{D}u, s_h^{n+1}), \tag{3.17}$$

where $\mathcal{D}q := q^{n+1} - q^n$ and $\mathcal{D}\omega := \omega^{n+1} - \omega^n$. For (3.12a) and (3.12b), taking the test functions as $\varphi_1 = \mathcal{D}u$ and $\theta_1 = \mathcal{D}\omega$, we have

$$\frac{1}{\Delta t}(\mathcal{D}u, \mathcal{D}u)_K = H_K^+(s_h^{n+1}, \mathcal{D}u) - \frac{a}{2}(q_h^{n+1}, \mathcal{D}u)_K - (r_h^{n+1}b_h^n, \mathcal{D}u)_K, \tag{3.18}$$

$$(s_h^{n+1}, \mathcal{D}\omega)_K = -H_K^-(q_h^{n+1}, \mathcal{D}\omega). \tag{3.19}$$

Now combining Eqs. (3.16)–(3.19), we find

$$\begin{aligned} &(\mathcal{D}q, q_h^{n+1})_K + \frac{1}{\Delta t}(\mathcal{D}u, \mathcal{D}u)_K + (r_h^{n+1}b_h^n, \mathcal{D}u)_K \\ &= -H_K^+(\mathcal{D}\omega, q_h^{n+1}) - H_K^-(q_h^{n+1}, \mathcal{D}\omega) + H_K^-(\mathcal{D}u, s_h^{n+1}) + H_K^+(s_h^{n+1}, \mathcal{D}u). \end{aligned} \tag{3.20}$$

Summing up (3.20) over K and by the property (2.4), we get

$$\int_{\Omega} \mathcal{D}q q_h^{n+1} dx + \frac{1}{\Delta t} \int_{\Omega} (\mathcal{D}u)^2 dx + \int_{\Omega} r_h^{n+1} b_h^n \mathcal{D}u dx = 0. \tag{3.21}$$

Multiplying the Eq. (3.13) with $2r_h^{n+1}$, we obtain

$$2r_h^{n+1}(r_h^{n+1} - r_h^n) = \int_{\Omega} r_h^{n+1} b_h^n \mathcal{D}u dx. \tag{3.22}$$

Combining Eqs. (3.21) and (3.22) and using the identity

$$a(a - b) = \frac{1}{2}(a^2 - b^2 + (a - b)^2),$$

we have the discrete energy stability

$$\frac{1}{2} \int_{\Omega} (q_h^{n+1})^2 dx + (r_h^{n+1})^2 + \frac{1}{\Delta t} \int_{\Omega} (\mathcal{D}u)^2 dx \leq \frac{1}{2} \int_{\Omega} (q_h^n)^2 dx + (r_h^n)^2.$$

□

Note that

$$\|u_h^{n+1}\|^2 \leq \|u_h^{n+1} - u_h^n\|^2 + \|u_h^n\|^2.$$

It follows from the discrete energy stability (3.15) that

$$\frac{1}{2} \|q_h^{n+1}\|^2 + (r_h^{n+1})^2 + \frac{1}{\Delta t} \|u_h^{n+1}\|^2 \leq \frac{1}{2} \|q_h^n\|^2 + (r_h^n)^2 + \frac{1}{\Delta t} \|u_h^n\|^2.$$

Then by special initial solutions, we can easily get

$$\|u_h^n\| \leq C, \quad \|u_h^n\|_{\infty} \leq C. \tag{3.23}$$

The second inequality can be proved by the essentially same procedure as that in Lemma 2.4.

3.3 Optimal Error Estimates of the Fully-Discrete LDG Scheme

To obtain the optimal error estimates of the first-order fully-discrete LDG scheme (3.12), we would like to introduce the elliptic projection [7], which plays an important role in our analysis. Firstly, we assume the exact solution of Eq. (1.3) is sufficiently smooth with bounded derivatives,

$$u \in L^{\infty}(0, T; H^{k+4}), \quad u_t \in L^{\infty}(0, T; H^{k+1}), \quad u_{tt} \in L^{\infty}(0, T; L^2). \tag{3.24}$$

Then suppose u, s, q, ω are the exact solution of the first order system (2.1), we define the elliptic projection $U_h, Q_h \in V_h, S_h, W_h \in \Sigma_h$ satisfying

$$H^+(S_h, \varphi_1) = H^+(s, \varphi_1), \tag{3.25a}$$

$$(S_h, \theta_1) + H^-(Q_h, \theta_1) = (s, \theta_1) + H^-(q, \theta_1), \tag{3.25b}$$

$$(Q_h, \varphi_2) + H^+(W_h, \varphi_2) = (q, \varphi_2) + H^+(\omega, \varphi_2), \tag{3.25c}$$

$$(W_h, \theta_2) + H^-(U_h, \theta_2) = (\omega, \theta_2) + H^-(u, \theta_2), \tag{3.25d}$$

for any $\varphi_1, \varphi_2 \in V_h, \theta_1, \theta_2 \in \Sigma_h$. Following [7], we assume $(u - U_h, 1) = 0$ to ensure the problem (3.25) is well-defined. In addition, we consider the adjoint problem

$$\theta = \nabla \sigma, \quad \varphi = \nabla \cdot \theta, \quad \zeta = \nabla \varphi, \quad z = \nabla \cdot \zeta, \tag{3.26}$$

and assume the elliptic regularity result (see, e.g., [7])

$$\|\zeta\|_{H^1(\Omega)} + \|\varphi\|_{H^2(\Omega)} + \|\theta\|_{H^3(\Omega)} + \|\sigma\|_{H^4(\Omega)} \leq C_* \|z\|, \tag{3.27}$$

then we derive the approximation property of the elliptic projection.

Lemma 3.2 *Suppose u, q are the exact solution of the first order system (2.1) and U_h, Q_h are the elliptic projection (3.25), there hold*

$$\|u - U_h\| + \|q - Q_h\| \leq Ch^{k+1}, \tag{3.28}$$

where $C > 0$ is independent of $h, \Delta t$, but depends on the regularity of u and the elliptic regularity constant C_* .

Remark 3.3 The proof will be obtained by the aid of the duality argument and the projections defined by (2.13)–(2.14) for the one-dimensional space and (2.15)–(2.16) for two-dimensional Cartesian meshes. It is very similar to [7], in which the L^2 projection for triangular meshes is considered and only the optimal error estimate of u in (3.28) is obtained. The details of the proof will be shown in the Appendix.

Denote the error between the exact solution and the numerical solution of the fully-discrete LDG scheme (3.12) by $e_u^n = u(x, t^n) - u_h^n, e_s^n = s(x, t^n) - s_h^n$. As usual, we divide the error into

$$e_u^n = u(x, t^n) - U_h^n + U_h^n - u_h^n = R_u^n + \xi_u^n, \quad e_s^n = s(x, t^n) - S_h^n + S_h^n - s_h^n = R_s^n + \xi_s^n,$$

where U_h^n, S_h^n are the elliptic projections (3.25) of $u(x, t^n)$ and $s(x, t^n)$, respectively. Similar notations are used for q and ω . By the approximation property in Lemma 3.2, we have

$$\|R_u^n\| + \|R_q^n\| \leq Ch^{k+1}, \quad \|R_u^{n+1} - R_u^n\| \leq C\Delta t h^{k+1}. \tag{3.29}$$

Next we consider the error equation of the fully-discrete LDG scheme (3.12). It is easy to verify that

$$u(t^{n+1}) = u(t^n) - \Delta t \nabla \cdot s(t^{n+1}) - \frac{a}{2} \Delta t q(t^{n+1}) - \Delta t r(t^{n+1})b(t^n) + \rho_1^n, \tag{3.30}$$

$$r(t^{n+1}) = r(t^n) + \frac{1}{2}(b(t^n), u(t^{n+1}) - u(t^n)) + \rho_2^n. \tag{3.31}$$

Here we omit the spacial variable x for simplicity and s, q are the auxiliary variables (2.1b)–(2.1d), $b(t^n) = \Phi'(u(t^n))/\sqrt{E_1(u(t^n)) + B}$. ρ_1 and ρ_2 are the local truncation errors in time satisfying

$$\|\rho_1^n\| \leq C(\Delta t)^2, \quad \|\rho_2^n\| \leq C(\Delta t)^2. \tag{3.32}$$

Multiply the test function $\varphi_1 \in V_h$ on both sides of (3.30) and integrate the equation by parts to yield

$$\begin{aligned} (u(t^{n+1}), \varphi_1) &= (u(t^n), \varphi_1) + \Delta t H^+(s(t^{n+1}), \varphi_1) - \frac{a}{2} \Delta t (q(t^{n+1}), \varphi_1) \\ &\quad - \Delta t (r(t^{n+1})b(t^n), \varphi_1) + (\rho_1^n, \varphi_1). \end{aligned}$$

Subtracting the above equation from the first equality of the scheme (3.12) gives the error equations for ξ_u^n as follows

$$\begin{aligned} (\xi_u^{n+1} - \xi_u^n, \varphi_1) &= -(R_u^{n+1} - R_u^n, \varphi_1) + \Delta t H^+(\xi_s^{n+1}, \varphi_1) - \frac{a}{2} \Delta t (e_q^{n+1}, \varphi_1) \\ &\quad - \Delta t (r(t^{n+1})b(t^n) - r_h^{n+1}b_h^n, \varphi_1) + (\rho_1^n, \varphi_1). \end{aligned} \tag{3.33}$$

Note that the auxiliary variables q, s, ω also satisfy the scheme (3.12) and we have

$$(\xi_s^{n+1}, \theta_1) = -H^-(\xi_q^{n+1}, \theta_1), \tag{3.34a}$$

$$(\xi_q^{n+1}, \varphi_2) = -H^+(\xi_\omega^{n+1}, \varphi_2) + \frac{a}{2}(e_u^{n+1}, \varphi_2), \tag{3.34b}$$

$$(\xi_\omega^{n+1}, \theta_2) = -H^-(\xi_u^{n+1}, \theta_2). \tag{3.34c}$$

Here we use the definition of the elliptic projection (3.25). For the error $e_r^n = r(t^n) - r^n$, we have

$$\begin{aligned} e_r^{n+1} &= e_r^n + \frac{1}{2}(b(t^n), u(t^{n+1}) - u(t^n)) - \frac{1}{2}(b_h^n, u_h^{n+1} - u_h^n) + \rho_2^n \\ &= e_r^n + \frac{1}{2}(b(t^n) - b_h^n, u(t^{n+1}) - u(t^n)) + \frac{1}{2}(b_h^n, e_u^{n+1} - e_u^n) + \rho_2^n. \end{aligned} \tag{3.35}$$

Now we give the optimal error estimates in the following theorem.

Theorem 3.4 *Let u_h^n be the numerical solution of the scheme (3.12), and u be the exact solution of equation (1.3). Suppose u satisfies the smoothness assumption (3.24), then there exists a constant $C > 0$ such that*

$$\|u(x, t^n) - u_h^n\| \leq C(h^{k+1} + \Delta t), \tag{3.36}$$

where C is independent of h and u_h^n and dependent on the regularity of u and C_* .

Proof Taking the test function $\varphi_1 = \xi_u^{n+1}$ in (3.33), we obtain the first energy equality in the form of ξ_u

$$\frac{1}{2}\|\xi_u^{n+1}\|^2 - \frac{1}{2}\|\xi_u^n\|^2 + \frac{1}{2}\|\xi_u^{n+1} - \xi_u^n\|^2 = \mathcal{T}_1 + \mathcal{T}_2 + \mathcal{T}_3,$$

where

$$\begin{aligned} \mathcal{T}_1 &= -(R_u^{n+1} - R_u^n, \xi_u^{n+1}) + (\rho_1^n, \xi_u^{n+1}), \\ \mathcal{T}_2 &= \Delta t H^+(\xi_s^{n+1}, \xi_u^{n+1}) - \frac{a}{2}\Delta t(e_q^{n+1}, \xi_u^{n+1}), \\ \mathcal{T}_3 &= -\Delta t(r(t^{n+1})b(t^n) - r_h^{n+1}b_h^n, \xi_u^{n+1}). \end{aligned}$$

The terms will be estimated separately. Adopting the Cauchy–Schwarz inequality, the property of the elliptic projection (3.29) and (3.32), we obtain

$$\mathcal{T}_1 \leq C\Delta th^{k+1}\|\xi_u^{n+1}\| + C(\Delta t)^2\|\xi_u^{n+1}\|. \tag{3.37}$$

For the second term, by (2.4) and (3.34), we have

$$\begin{aligned} H^+(\xi_s^l, \xi_u^m) &= -H^-(\xi_u^m, \xi_s^l) = (\xi_\omega^m, \xi_s^l) = -H^-(\xi_q^l, \xi_\omega^m) \\ &= H^+(\xi_\omega^m, \xi_q^l) = -(\xi_q^m, \xi_q^l) + \frac{a}{2}(e_u^m, \xi_q^l), \quad \forall m, l = n, n + 1. \end{aligned} \tag{3.38}$$

Thus

$$\begin{aligned} \mathcal{T}_2 &= -\Delta t\|\xi_q^{n+1}\|^2 + \frac{a}{2}\Delta t(e_u^{n+1}, \xi_q^{n+1}) - \frac{a}{2}\Delta t(e_q^{n+1}, \xi_u^{n+1}) \\ &= -\Delta t\|\xi_q^{n+1}\|^2 + \frac{a}{2}\Delta t(R_u^{n+1}, \xi_q^{n+1}) - \frac{a}{2}\Delta t(R_q^{n+1}, \xi_u^{n+1}) \\ &\leq -\Delta t\|\xi_q^{n+1}\|^2 + C\Delta th^{k+1}(\|\xi_q^{n+1}\| + \|\xi_u^{n+1}\|), \end{aligned} \tag{3.39}$$

where the property (3.29) is used. For the nonlinear term, we can obtain

$$\begin{aligned} \mathcal{T}_3 &= -\Delta t (r(t^{n+1})(b(t^n) - b_h^n), \xi_u^{n+1}) - \Delta t \left((r(t^{n+1}) - r_h^{n+1})b_h^n, \xi_u^{n+1} \right) \\ &\leq \Delta t |r(t^{n+1})| \|b(t^n) - b_h^n\| \|\xi_u^{n+1}\| + \Delta t |e_r^{n+1}| \|b_h^n\| \|\xi_u^{n+1}\|. \end{aligned}$$

With the definition of $b(t^n)$, b_h^n and through some calculations, we derive

$$\begin{aligned} b(t^n) - b_h^n &= \frac{\Phi'(u(t^n))}{\sqrt{E_1(u(t^n)) + B}} - \frac{\Phi'(u_h^n)}{\sqrt{E_1(u_h^n) + B}} \\ &= \frac{\Phi'(u_h^n)}{\sqrt{E_1(u_h^n) + B} \sqrt{E_1(u(t^n)) + B}} \frac{E_1(u_h^n) - E_1(u(t^n))}{\sqrt{E_1(u_h^n) + B} + \sqrt{E_1(u(t^n)) + B}} \\ &\quad + \frac{\Phi'(u(t^n)) - \Phi'(u_h^n)}{\sqrt{E_1(u(t^n)) + B}}, \end{aligned}$$

which leads to

$$\begin{aligned} \|b(t^n) - b_h^n\| &\leq C \|\Phi'(u(t^n)) - \Phi'(u_h^n)\| + C \|E_1(u_h^n) - E_1(u(t^n))\| \\ &\leq C \|\Phi''(\eta_1)(u(t^n) - u_h^n)\| + C \|\Phi'(\eta_2)(u_h^n - u(t^n))\| \\ &\leq C (\|R_u^n\| + \|\xi_u^n\|). \end{aligned} \tag{3.40}$$

Here the first and last inequalities have used the boundness (3.23) and η_1, η_2 lie between u_h^n and $u(t^n)$. It follows from $r(t^{n+1}) < C$ and (3.29) that

$$\mathcal{T}_3 \leq C \Delta t (h^{k+1} + \|\xi_u^n\|) \|\xi_u^{n+1}\| + \Delta t \|b_h^n\| |e_r^{n+1}| \|\xi_u^{n+1}\|. \tag{3.41}$$

Combine the estimates (3.37)–(3.41) to yield

$$\frac{1}{2} \|\xi_u^{n+1}\|^2 - \frac{1}{2} \|\xi_u^n\|^2 + \frac{1}{2} \|\xi_u^{n+1} - \xi_u^n\|^2 \leq \mathcal{R}_1 \tag{3.42}$$

where

$$\begin{aligned} \mathcal{R}_1 &= -\Delta t \|\xi_q^{n+1}\|^2 + C \Delta t h^{k+1} \|\xi_q^{n+1}\| + C \Delta t (h^{k+1} + \|\xi_u^n\| + \Delta t) \|\xi_u^{n+1}\| \\ &\quad + \Delta t \|b_h^n\| |e_r^{n+1}| \|\xi_u^{n+1}\| \\ &\leq \Delta t \|\xi_u^{n+1}\|^2 - \frac{1}{2} \Delta t \|\xi_q^{n+1}\|^2 + \frac{1}{2} \Delta t \|b_h^n\|^2 |e_r^{n+1}|^2 + C \Delta t (h^{2k+2} + \|\xi_u^n\|^2 + (\Delta t)^2). \end{aligned}$$

Taking the test function $\varphi_1 = (\xi_u^{n+1} - \xi_u^n)/\Delta t$ in (3.33), multiplying $2e_r^{n+1}$ on both sides of (3.35) and adding them together, we obtain the second energy equality

$$\frac{1}{\Delta t} \|\xi_u^{n+1} - \xi_u^n\|^2 + (e_r^{n+1})^2 - (e_r^n)^2 + (e_r^{n+1} - e_r^n)^2 = \mathcal{L}_1 + \mathcal{L}_2 + \mathcal{L}_3 + \mathcal{L}_4,$$

where

$$\begin{aligned} \mathcal{L}_1 &= -\frac{1}{\Delta t} (R_u^{n+1} - R_u^n, \xi_u^{n+1} - \xi_u^n) + \frac{1}{\Delta t} (\rho_1^n, \xi_u^{n+1} - \xi_u^n) + 2\rho_2^n e_r^{n+1}, \\ \mathcal{L}_2 &= H^+(\xi_s^{n+1}, \xi_u^{n+1} - \xi_u^n) - \frac{a}{2} (e_q^{n+1}, \xi_u^{n+1} - \xi_u^n), \\ \mathcal{L}_3 &= -(r(t^{n+1})b(t^n) - r_h^{n+1}b_h^n, \xi_u^{n+1} - \xi_u^n) + e_r^{n+1} (b_h^n, e_u^{n+1} - e_u^n), \\ \mathcal{L}_4 &= e_r^{n+1} (b(t^n) - b_h^n, u(t^{n+1}) - u(t^n)). \end{aligned}$$

Using the Cauchy–Schwarz inequality and the approximation properties (3.29), (3.32), we have

$$\mathcal{L}_1 \leq Ch^{k+1} \|\xi_u^{n+1} - \xi_u^n\| + C\Delta t \|\xi_u^{n+1} - \xi_u^n\| + C(\Delta t)^2 |e_r^{n+1}|. \tag{3.43}$$

By the property (3.38), we derive

$$\begin{aligned} \mathcal{L}_2 &= -(\xi_q^{n+1} - \xi_q^n, \xi_q^{n+1}) + \frac{a}{2}(e_u^{n+1} - e_u^n, \xi_q^{n+1}) - \frac{a}{2}(e_q^{n+1}, \xi_u^{n+1} - \xi_u^n) \\ &= -(\xi_q^{n+1} - \xi_q^n, \xi_q^{n+1}) + \frac{a}{2}(R_u^{n+1} - R_u^n, \xi_q^{n+1}) - \frac{a}{2}(R_q^{n+1}, \xi_u^{n+1} - \xi_u^n) \\ &\leq -(\xi_q^{n+1} - \xi_q^n, \xi_q^{n+1}) + Ch^{k+1}(\Delta t \|\xi_q^{n+1}\| + \|\xi_u^{n+1} - \xi_u^n\|), \end{aligned} \tag{3.44}$$

where the approximation property (3.29) of the elliptic is used again. For the term \mathcal{L}_3 , some calculations yield

$$\begin{aligned} \mathcal{L}_3 &= -(r(t^{n+1})(b(t^n) - b_h^n), \xi_u^{n+1} - \xi_u^n) - (e_r^{n+1} b_h^n, \xi_u^{n+1} - \xi_u^n) + e_r^{n+1}(b_h^n, e_u^{n+1} - e_u^n) \\ &\leq |r(t^{n+1})| \|b(t^n) - b_h^n\| \|\xi_u^{n+1} - \xi_u^n\| + |e_r^{n+1}| \|b_h^n\| \|R_u^{n+1} - R_u^n\| \\ &\leq C(h^{k+1} + \|\xi_u^n\|) \|\xi_u^{n+1} - \xi_u^n\| + C\Delta t h^{k+1} |e_r^{n+1}|. \end{aligned} \tag{3.45}$$

Here we use the estimate (3.40) and (3.29). Similarly, we have

$$\mathcal{L}_4 \leq C|e_r^{n+1}|(h^{k+1} + \|\xi_u^n\|) \|u(t^{n+1}) - u(t^n)\| \leq C\Delta t |e_r^{n+1}|(h^{k+1} + \|\xi_u^n\|). \tag{3.46}$$

Then by the estimates (3.43)–(3.46), the second the energy equality turns out to be

$$LHS \leq \mathcal{R}_2, \tag{3.47}$$

where

$$\begin{aligned} LHS &= \frac{1}{\Delta t} \|\xi_u^{n+1} - \xi_u^n\|^2 + (e_r^{n+1})^2 - (e_r^n)^2 + (e_r^{n+1} - e_r^n)^2 \\ &\quad + \frac{1}{2} \|\xi_q^{n+1}\|^2 - \frac{1}{2} \|\xi_q^n\|^2 + \frac{1}{2} \|\xi_q^{n+1} - \xi_q^n\|^2, \\ \mathcal{R}_2 &= C(h^{k+1} + \Delta t + \|\xi_u^n\|) \|\xi_u^{n+1} - \xi_u^n\| + Ch^{k+1} \Delta t \|\xi_q^{n+1}\| \\ &\quad + C\Delta t(h^{k+1} + \|\xi_u^n\| + \Delta t) |e_r^{n+1}| \\ &\leq \frac{1}{\Delta t} \|\xi_u^{n+1} - \xi_u^n\|^2 + \frac{1}{2} \Delta t \|\xi_q^{n+1}\|^2 + \frac{1}{2} \Delta t |e_r^{n+1}|^2 \\ &\quad + C\Delta t(h^{2k+2} + (\Delta t)^2 + \|\xi_u^n\|^2). \end{aligned}$$

Note that

$$\|\xi_u^{n+1}\|^2 \leq 2(\|\xi_u^n\|^2 + \|\xi_u^{n+1} - \xi_u^n\|^2), \quad |e_r^{n+1}|^2 \leq 2(|e_r^n|^2 + (e_r^{n+1} - e_r^n)^2).$$

Add the energy inequalities (3.42), (3.47) together to get

$$\begin{aligned} &\|\xi_u^{n+1}\|^2 - \|\xi_u^n\|^2 + \|\xi_u^{n+1} - \xi_u^n\|^2 + 2(e_r^{n+1})^2 - 2(e_r^n)^2 + 2(e_r^{n+1} - e_r^n)^2 \\ &\quad + \|\xi_q^{n+1}\|^2 - \|\xi_q^n\|^2 + \|\xi_q^{n+1} - \xi_q^n\|^2 \leq \mathcal{R}_3, \end{aligned}$$

where

$$\begin{aligned} \mathcal{R}_3 &\leq 4\Delta t \|\xi_u^{n+1} - \xi_u^n\|^2 + 2\Delta t(1 + \|b_h^n\|^2) |e_r^{n+1} - e_r^n|^2 \\ &\quad + C\Delta t(h^{2k+2} + (\Delta t)^2 + \|\xi_u^n\|^2 + (e_r^n)^2). \end{aligned}$$

If

$$4\Delta t < 1, \quad \Delta t(1 + \|b_h^n\|^2) < 1,$$

we can get the estimate by using the discrete Gronwall’s inequality

$$\|\xi_u^n\|^2 + \|\xi_q^n\|^2 + 2(e_r^n)^2 \leq C(h^{2k+2} + (\Delta t)^2).$$

By the triangle inequality and (3.29), we complete the proof. □

3.4 The Semi-implicit SDC Method

The linear scheme proposed above is unconditionally energy stable. However, it is only first-order accurate in time, while the LDG method is high-order accurate in space. To obtain high-order accuracy in both space and time, we will employ the semi-implicit SDC method iteratively to improve the temporal accuracy.

The semi-implicit SDC method is based on a first-order scheme, for example the SAV method (3.12) here. An advantage of the SDC method is that it is a one step method and can be constructed easily and systematically for any order of accuracy. More details for the semi-implicit SDC method can be found in [16, 26].

We do the SDC procedure in every interval $[t^n, t^{n+1}]$. We divide the time interval $[t^n, t^{n+1}]$ into P subintervals by choosing the points $t^{n,m}$ for $m = 0, 1, \dots, P$ such that $t^n = t^{n,0} < t^{n,1} < \dots < t^{n,m} < \dots < t^{n,P} = t^{n+1}$. Let $\Delta t^{n,m} = t^{n,m+1} - t^{n,m}$ and $u_k^{n,m}$ denotes the k th order approximation to $u(t^{n,m})$. The points $\{t^{n,m}\}_{m=0}^P$ can be chosen to be the Chebyshev Gauss–Lobatto nodes on $[t^n, t^{n+1}]$ to avoid the instability of approximation at equispaced nodes for high order accuracy. Starting from u^n and r^n , we give the algorithm to calculate u^{n+1} and r^{n+1} in the following.

Compute the initial approximation

$$u_1^{n,0} = u^n \text{ and } r_1^{n,0} = r^n.$$

Use the first-order scheme (3.12) to compute a first-order accurate approximate solution u_1 and r_1 at the nodes $\{t^{n,m}\}_{m=1}^P$, i.e.

For $m = 0, \dots, P - 1$

$$u_1^{n,m+1} = u_1^{n,m} + \Delta t^{n,m} \left(- \left(\Delta + \frac{a}{2} \right)^2 u_1^{n,m+1} - \frac{r_1^{n,m+1}}{\sqrt{E_1(u_1^{n,m} + B)}} \Phi'(u_1^{n,m}) \right), \quad (3.48)$$

$$r_1^{n,m+1} = r_1^{n,m} + \frac{1}{2\sqrt{E_1(u_1^{n,m}) + B}} \int_{\Omega} \Phi'(u_1^{n,m})(u_1^{n,m+1} - u_1^{n,m}) dx. \quad (3.49)$$

Compute successive corrections

For $k = 1, \dots, K$

$$u_{k+1}^{n,0} = u^n \text{ and } r_{k+1}^{n,0} = r^n.$$

For $m = 0, \dots, P - 1$

$$\begin{aligned}
 u_{k+1}^{n,m+1} = & u_{k+1}^{n,m} + \Delta t^{n,m} \left(- \left(\Delta + \frac{a}{2} \right)^2 u_{k+1}^{n,m+1} - \frac{r_{k+1}^{n,m}}{\sqrt{E_1(u_{k+1}^{n,m}) + B}} \Phi'(u_{k+1}^{n,m}) \right. \\
 & \left. + \left(\Delta + \frac{a}{2} \right)^2 u_k^{n,m+1} + \frac{r_k^{n,m}}{\sqrt{E_1(u_k^{n,m}) + B}} \Phi'(u_k^{n,m}) \right) + I_m^{m+1}(F(u_k, r_k)), \quad (3.50)
 \end{aligned}$$

$$r_{k+1}^{n,m+1} = \sqrt{E_1(u_{k+1}^{n,m+1}) + B}, \quad (3.51)$$

where

$$F(u_k, r_k) = - \left(\Delta + \frac{a}{2} \right)^2 u_k - \frac{r_k}{\sqrt{E_1(u_k) + B}} \Phi'(u_k).$$

Here, $I_m^{m+1}(F(u_k, r_k))$ is the integral of the P -th degree interpolating polynomial on the $P + 1$ points $(t^{n,m}, F(u_k^{n,m}, r_k^{n,m}))_{m=0}^P$ over the subinterval $[t^{n,m}, t^{n,m+1}]$, which is the numerical quadrature approximation of

$$\int_{t^{n,m}}^{t^{n,m+1}} F(u(t), r(t)) dt.$$

Finally we have $u^{n+1} = u_{K+1}^{n,P}$ and $r^{n+1} = r_{K+1}^{n,P}$.

Remark 3.5 (*Local truncation error*) The local truncation error obtained with the above semi-implicit SDC scheme [26] is

$$\mathcal{O}(\tau^{\min[K+1, P+1]}),$$

where $\tau = \max_{n,m} \Delta t^{n,m}$.

4 Numerical Experiments

In this section, we present some numerical experiments using the LDG spatial discretization and the semi-implicit SDC temporal discretization for the Swift–Hohenberg equation. In all examples, we assume periodic boundary conditions. We first perform an accuracy test, which shows the expected accuracy in time and space. Then, we present an example to show the energy stability of the first-order scheme and the semi-implicit SDC scheme, and to illustrate the advantage of the high-order SDC method. Lastly, we present some long time simulations to verify the energy stability and show the effectiveness of the proposed schemes.

Example 4.1 (*Accuracy tests and efficiency of the proposed numerical methods*) Consider the Swift–Hohenberg equation in the square domain $\Omega = [0, 2\pi]^2$. For the tests, we choose a suitable source term such that the exact solution is taken as

$$u(x, y, t) = e^{-2t} \sin(x) \sin(y).$$

Choose the parameters $\varepsilon = 0.025$, $g = 0$ and $a = 2$.

To test the temporal accuracy of the first-order scheme (3.12), we use the meshes $N = 64$ and \mathcal{P}^2 approximation to ensure that the spatial discretization error is small enough, and the temporal discretization error is dominant in the numerical test. The time step refinement path

Table 1 Temporal accuracy test

m	L^2 error	Order	L^∞ error	Order
1	2.24E-03	–	7.83E-04	–
2	1.10E-03	1.03	3.83E-04	1.03
3	5.47E-04	1.01	1.96E-04	0.97
4	2.75E-04	0.99	1.02E-04	0.94

L^2 and L^∞ errors and orders of convergence at $T = 0.1$. The time step refinement path is taken to be $\Delta t = \Delta t_0/2^m$, $\Delta t_0 = 0.1$ and $m = 1, 2, 3, 4$

Table 2 Spatial accuracy test. L^2 and L^∞ errors and orders of convergence at $T = 0.1$

	N	L^2 error	Order	L^∞ error	Order
\mathcal{P}^1	8	1.86E-01	–	1.25E-01	–
	16	4.72E-02	1.98	3.36E-02	1.90
	32	1.18E-02	1.99	8.56E-03	1.98
	64	2.96E-03	2.00	2.15E-03	1.99
\mathcal{P}^2	8	2.39E-02	–	2.28E-02	–
	16	3.00E-03	2.99	2.82E-03	3.02
	32	3.76E-04	3.00	3.48E-04	3.02
	64	4.76E-05	2.98	4.48E-05	2.96

The mesh size refinement path is taken to be $\Delta x = \Delta y = 2\pi/N$ with $N = 8, 16, 32, 64$

Table 3 Spatial and temporal accuracy test. L^2 and L^∞ errors and orders of convergence at $T = 0.5$ with $\Delta t = 0.2\Delta x$

	N	L^2 error	Order	L^∞ error	Order
\mathcal{P}^1	8	8.42E-02	–	5.83E-02	–
	16	2.12E-02	1.99	1.52E-02	1.93
	32	5.33E-03	2.00	3.85E-03	1.98
	64	1.33E-03	2.00	9.66E-04	2.00
\mathcal{P}^2	8	1.16E-02	–	9.79E-03	–
	16	1.38E-03	3.06	1.23E-03	2.99
	32	1.70E-04	3.02	1.54E-04	3.00
	64	2.12E-05	3.00	1.93E-05	2.99

Table 4 Total CPU time for the Swift–Hohenberg equation using various time-stepping methods

	Third-order SDC method	First-order method
CPU time	158 s	3414 s

is taken to be $\Delta t = \Delta t_0/2^m$, $\Delta t_0 = 0.1$ and $m = 1, 2, 3, 4$. The L^2 and L^∞ errors and orders of convergence are presented in Table 1, which shows first-order accurate in time and agrees with the theoretical result.

To test the spatial accuracy numerically, we set the time step as $\Delta t = 10^{-4}$ to ensure that the spatial discretization error is dominant. The mesh sizes are set to be $\Delta x = \Delta y = 2\pi/N$ with $N = 8, 16, 32, 64$. The L^2 and L^∞ errors and convergence rate at $T = 0.1$ are reported

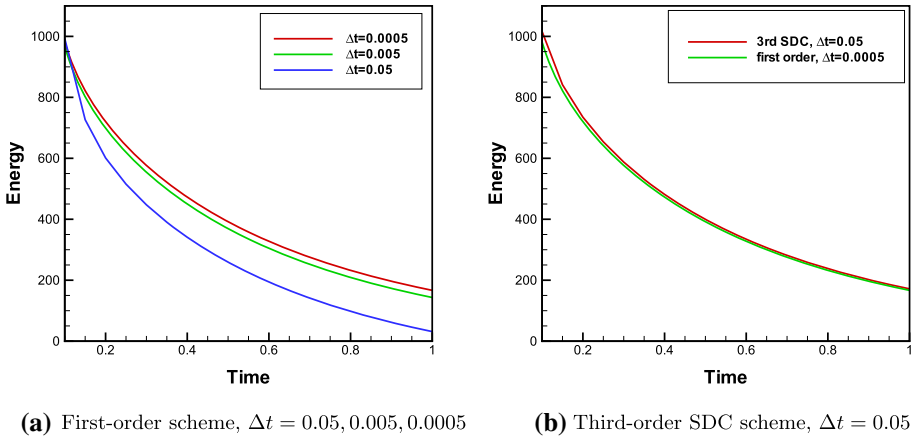


Fig. 1 Energy evolution of the first-order scheme and the third-order semi-implicit SDC scheme

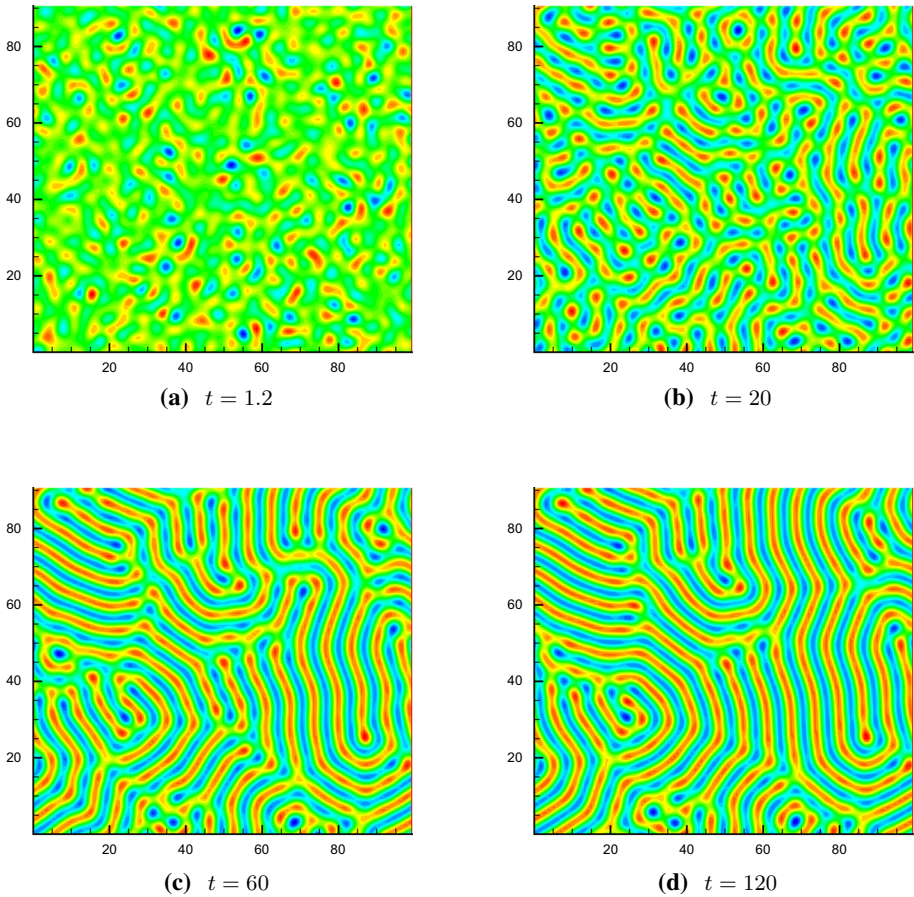


Fig. 2 Numerical results of the Swift-Hohenberg equation using the third-order SDC method and the piecewise \mathcal{P}^2 polynomial basis with $\varepsilon = 0.3, g = 0.0$

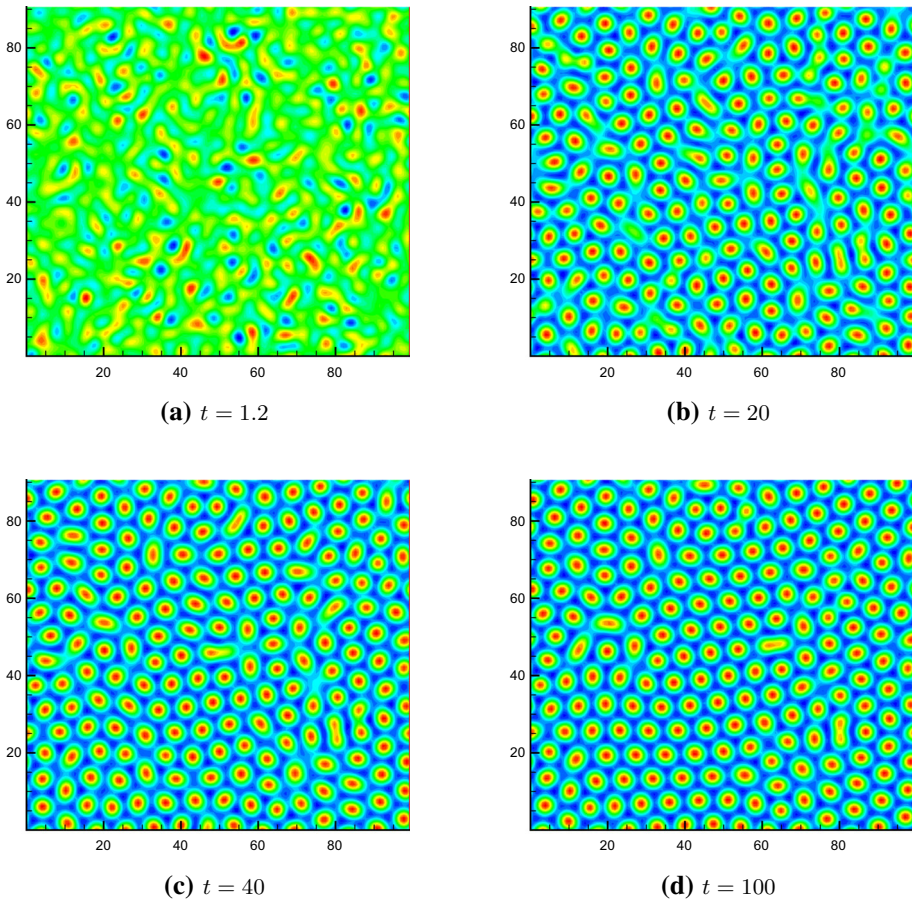


Fig. 3 Numerical results of the Swift–Hohenberg equation using the third-order SDC method and the piecewise \mathcal{P}^2 polynomial basis with $\varepsilon = 0.1, g = 1.0$

in Table 2, which shows $(k + 1)$ -th orders of accuracy for \mathcal{P}^k approximation and agrees with the theoretical result.

The L^2 and L^∞ errors and accuracy of the third-order SDC scheme are presented in Table 3. The error is expected to be at the order of $\min\{\mathcal{O}(\Delta t^3), \mathcal{O}(\Delta x^{k+1})\}$ for \mathcal{P}^k approximation. Namely, high order accuracy in both space and time is easy to achieve for our proposed LDG and SDC methods with larger time step sizes.

For the sake of comparison of efficiency, we document the CPU time of the third-order SDC method and the first-order method for solving the Swift–Hohenberg equation. We choose \mathcal{P}^2 polynomial for spatial discretization, and the suitably chosen Δt which yields an L^∞ error at the level of 10^{-5} for both methods. The results are contained in Table 4. Comparing the CPU times, we notice that the third-order SDC method requires less time.

Example 4.2 (Energy stability test) In this example, we perform stability tests to verify the energy stability, the initial condition is taken as

$$u(x, y, 0) = rand(x, y),$$

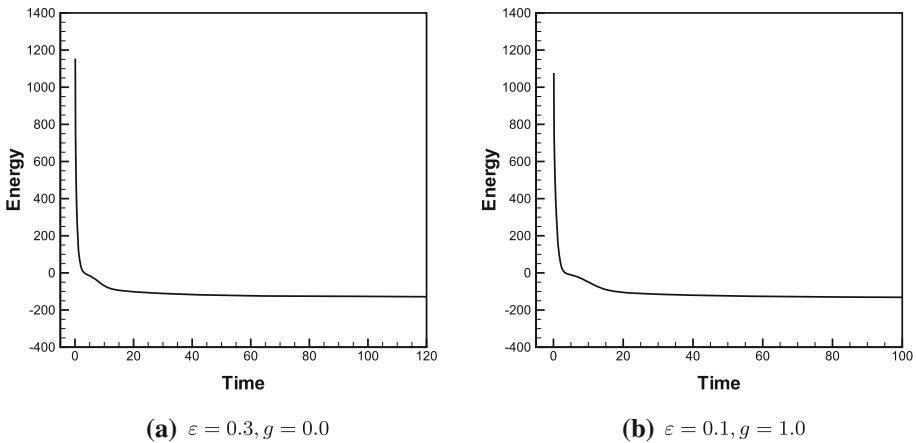


Fig. 4 Energy evolution of the third-order SDC method

where $rand(x, y)$ is a random number between 0 and 1. The computational domain is $\Omega = [0, 100]^2$. Choose the parameters $\varepsilon = 0.3, g = 0$ and $a = 2$.

Figure 1a presents the energy evolution of the first-order scheme (3.12) with three different time step sizes, i.e. $\Delta t = 0.05, 0.005, 0.0005$. We can see the energy curves decay with all time step sizes, which agrees with the theoretical result of the unconditional energy stability. In addition, the energy curves are far away from the energy trace with $\Delta t = 0.0005$ if we use $\Delta t = 0.05, 0.005$ due to the low-accuracy of the first-order scheme (3.12). Thus, to obtain more accurate numerical solutions, a smaller time step is necessary. However, our semi-implicit SDC scheme can enhance the accuracy, we can see from Fig. 1b that the energy curve of the third-order SDC scheme with $\Delta t = 0.05$ is better coincident with the energy trace with $\Delta t = 0.0005$.

Example 4.3 (Long time simulations) In this example, we will show the long time simulations of the Swift–Hohenberg equation with the random initial data between 0 and 1. The computational domain is $\Omega = [0, 100]^2$. We take $a = 2$. For other parameters, we use the values $\varepsilon = 0.3, g = 0.0$ and $\varepsilon = 0.1, g = 1.0$, separately.

We adopt the third-order SDC method and the piecewise \mathcal{P}^2 polynomial basis. The computed mesh is composed of 128×128 elements with uniform mesh. The time step is $\Delta t = 0.05$. In Fig. 2, we show the contour plots of u with $\varepsilon = 0.3, g = 0.0$. While for $\varepsilon = 0.1, g = 1.0$, the corresponding results are contained in Fig. 3. The numerical results compare very well with the numerical calculations performed by Liu and Yin [15].

The energy evolution for both cases are presented in Fig. 4, we can see the energy is decreasing in time, which shows that the SDC method based on the first-order SAV scheme can maintain the energy stability.

5 Concluding Remarks

In this paper, we studied the LDG method for the Swift–Hohenberg equation and proved the energy stability for the semi-discrete and fully-discrete schemes. In addition, we derived the

optimal convergence rates for the semi-discrete and fully-discrete LDG schemes. The LDG methods are high-order accurate in space, while the proposed linear scheme is only first-order accurate in time, which motivates us to develop high-order temporal discretization methods. Thus, we employed the semi-implicit SDC method to improve the temporal accuracy based on the first-order SAV scheme. Numerical experiments verified the theoretical analysis and capabilities of the LDG and semi-implicit SDC methods.

Funding This work is supported by National Natural Science Foundation of China (Grant No. 12001171), Natural Science Foundation of Henan Province, China (Grant No. 222300420550).

Data availability Enquiries about data availability should be directed to the authors.

Declarations

Conflict of interest The authors declare that they have no conflict of interest.

6 Appendix

In this section, we will present the proof of Lemma 3.2, the optimal error estimate of the elliptic projection, by two lemmas. Denote the errors between the exact solutions of (2.1) and the elliptic projection (3.25) by R_u, R_ω, R_q, R_s . Suppose $(P, \Pi) = (P^-, P^+)$ is defined by (2.13)–(2.14) for the one-dimensional space, and take $(P, \Pi) = (P^-, P^+)$ defined by (2.15)–(2.16) for multidimensional Cartesian meshes. Then the errors can be divided into

$$\begin{aligned}
 R_u &= u - Pu + PR_u = \eta_u + PR_u, & R_\omega &= \omega - \Pi\omega + \Pi R_\omega = \eta_\omega + \Pi R_\omega, \\
 R_q &= q - Pq + PR_q = \eta_q + PR_q, & R_s &= s - \Pi s + \Pi R_s = \eta_s + \Pi R_s.
 \end{aligned}$$

With the definition of the elliptic projection (3.25) and the property (2.17), we obtain the error equation

$$0 = H^+(\Pi R_s, \varphi_1), \tag{6.1a}$$

$$(R_s, \theta_1) = -H^-(\eta_q, \theta_1) - H^-(PR_q, \theta_1), \tag{6.1b}$$

$$(R_q, \varphi_2) = -H^+(\Pi R_\omega, \varphi_2), \tag{6.1c}$$

$$(R_\omega, \theta_2) = -H^-(\eta_u, \theta_2) - H^-(PR_u, \theta_2). \tag{6.1d}$$

Note that for the one-dimensional space, $H^-(\eta_q, \theta_1) = 0$ and $H^-(\eta_u, \theta_2)$. The analysis will be the same as that in [25]. Now we show the following estimates.

Lemma 6.1

$$\begin{aligned}
 \|\Pi R_s\| &\lesssim h^{k+1}, & \|R_s\| + h^{1/2}\|R_s \cdot \mathbf{n}\|_{\varepsilon_h} &\lesssim h^{k+1}, \\
 \|PR_q\| &\lesssim \|PR_u\| + h^{k+1}, & \|R_q\| &\lesssim \|PR_u\| + h^{k+1}, \\
 \|\Pi R_\omega\| &\lesssim \|PR_u\| + h^{k+1}, & \|R_\omega\| + h^{1/2}\|R_\omega \cdot \mathbf{n}\|_{\varepsilon_h} &\lesssim \|PR_u\| + h^{k+1}.
 \end{aligned}$$

Here and below the notation $a \lesssim b$ means that, there exists a constant $C > 0$ such that $a \leq b$.

Proof Taking $\theta_1 = \Pi R_s$ in (6.1b) and by the property (2.4), (6.1a), we have

$$\begin{aligned}
 (R_s, \Pi R_s) &= -H^-(\eta_q, \Pi R_s) - H^-(PR_q, \Pi R_s) \\
 &= -H^-(\eta_q, \Pi R_s) + H^+(\Pi R_s, PR_q) = -H^-(\eta_q, \Pi R_s),
 \end{aligned}$$

which yields

$$\begin{aligned} \|\Pi R_s\|^2 &= (\Pi R_s, \Pi R_s - R_s) + (R_s, \Pi R_s) \\ &= (\Pi R_s, -\eta_s) - H^-(\eta_q, \Pi R_s) \\ &\lesssim h^{k+1} \|\Pi R_s\|. \end{aligned}$$

Here we use the approximation properties (2.18) and (2.19). Thus by the trace inequality and the triangle inequality, we have

$$\|\Pi R_s\| + h^{1/2} \|\Pi R_s \cdot \mathbf{n}\|_{\varepsilon_h} \lesssim h^{k+1}, \quad \|R_s\| + h^{1/2} \|R_s \cdot \mathbf{n}\|_{\varepsilon_h} \lesssim h^{k+1}.$$

Taking $\varphi_2 = PR_q$ in (6.1c) and by (2.4) and (6.1b), we obtain

$$\begin{aligned} (R_q, PR_q) &= -H^+(\Pi R_\omega, PR_q) = H^-(PR_q, \Pi R_\omega) \\ &= -H^-(\eta_q, \Pi R_\omega) - (R_s, \Pi R_\omega). \end{aligned}$$

Then

$$\begin{aligned} \|PR_q\|^2 &= (PR_q, PR_q - R_q) + (R_q, PR_q) \\ &= (PR_q, -\eta_q) - H^-(\eta_q, \Pi R_\omega) - (R_s, \Pi R_\omega) \\ &\leq \frac{1}{2} \|PR_q\|^2 + \frac{1}{2} \|\Pi R_\omega\|^2 + Ch^{2k+2}, \end{aligned}$$

where the Young’s inequality and (2.18)–(2.19) are used. Hence, we get

$$\|PR_q\| \lesssim \|\Pi R_\omega\| + h^{k+1}, \quad \|R_q\| \lesssim \|\Pi R_\omega\| + h^{k+1}. \tag{6.2}$$

Finally, we take $\theta_2 = \Pi R_\omega$ in (6.1d) and apply (2.4), (6.1c) to derive

$$\begin{aligned} (R_\omega, \Pi R_\omega) &= -H^-(\eta_u, \Pi R_\omega) - H^-(PR_u, \Pi R_\omega) \\ &= -H^-(\eta_u, \Pi R_\omega) - (R_q, PR_u). \end{aligned}$$

Then by Cauchy–Schwarz inequality, the Young’s inequality and (2.18)–(2.19), we have

$$\begin{aligned} \|\Pi R_\omega\|^2 &= (\Pi R_\omega, \Pi R_\omega - R_\omega) + (R_\omega, \Pi R_\omega) \\ &= (\Pi R_\omega, -\eta_\omega) - H^-(\eta_u, \Pi R_\omega) - (R_q, PR_u) \\ &\leq \frac{1}{2} \|\Pi R_\omega\|^2 + \|PR_u\|^2 + Ch^{2k+2}, \end{aligned}$$

which yields

$$\|\Pi R_\omega\| \lesssim \|PR_u\| + h^{k+1}, \quad \|R_\omega\| \lesssim \|PR_u\| + h^{k+1}.$$

It follows from (6.2) that

$$\|PR_q\| \lesssim \|PR_u\| + h^{k+1}, \quad \|R_q\| \lesssim \|PR_u\| + h^{k+1}.$$

A simple use of the trace inequality and the triangle inequality gives

$$h^{1/2} \|\Pi R_\omega \cdot \mathbf{n}\|_{\varepsilon_h} \lesssim \|PR_u\| + h^{k+1}, \quad h^{1/2} \|R_\omega \cdot \mathbf{n}\|_{\varepsilon_h} \lesssim \|PR_u\| + h^{k+1}.$$

The proof is completed. □

With the help of the adjoint problem (3.26), we will show the second lemma, which is used for the estimate of PR_u .

Lemma 6.2 For $z \in L^2(\Omega)$, we get

$$\begin{aligned}
 (PR_u, z) &= -H^-(\eta_u, \Pi\xi) - H^-(\eta_q, \Pi\theta) \\
 &\quad - (R_\omega, \Pi\xi - \xi) + (R_q, P\varphi - \varphi) - (R_s, \Pi\theta - \theta) \\
 &\quad + (\varphi - P\varphi, \nabla \cdot R_\omega) + (\sigma - P\sigma, \nabla \cdot R_s) \\
 &\quad - \langle (R_\omega - \hat{R}_\omega) \cdot \mathbf{n}, \varphi - P\varphi \rangle - \langle (R_s - \hat{R}_s) \cdot \mathbf{n}, \sigma - P\sigma \rangle. \tag{6.3}
 \end{aligned}$$

Proof By the adjoint problem (3.26) and integrating by part, we have

$$\begin{aligned}
 (PR_u, z) &= (PR_u, \nabla \cdot \xi) = -(\xi, \nabla PR_u) + \langle \xi \cdot \mathbf{n}, PR_u \rangle \\
 &= -H^+(\xi, PR_u) - \langle (\hat{\xi} - \xi) \cdot \mathbf{n}, PR_u \rangle \\
 &= -H^+(\xi - \Pi\xi, PR_u) - H^+(\Pi\xi, PR_u) \\
 &= H^-(PR_u, \Pi\xi). \tag{6.4}
 \end{aligned}$$

Here the second line uses the definition of H^+ , the third line holds since ξ is continuous across the element interface and we adopt the property (2.17) of Π as well as (2.4) for the last line. By (6.1d), we obtain

$$\begin{aligned}
 H^-(PR_u, \Pi\xi) &= -H^-(\eta_u, \Pi\xi) - (R_\omega, \Pi\xi) = -H^-(\eta_u, \Pi\xi) - (R_\omega, \Pi\xi - \xi) - (R_\omega, \xi).
 \end{aligned}$$

Similarly as (6.4), we derive

$$\begin{aligned}
 -(R_\omega, \xi) &= -(R_\omega, \nabla\varphi) = -(R_\omega, \nabla(\varphi - P\varphi)) - (R_\omega, \nabla P\varphi) \\
 &= (\nabla \cdot R_\omega, \varphi - P\varphi) - \langle R_\omega \cdot \mathbf{n}, \varphi - P\varphi \rangle \\
 &\quad - H^+(R_\omega, P\varphi) - \langle \hat{R}_\omega \cdot \mathbf{n}, P\varphi \rangle \\
 &= (\nabla \cdot R_\omega, \varphi - P\varphi) - \langle (R_\omega - \hat{R}_\omega) \cdot \mathbf{n}, \varphi - P\varphi \rangle \\
 &\quad + (R_q, P\varphi - \varphi) + (R_q, \varphi), \tag{6.5}
 \end{aligned}$$

where the second line holds by integrating by parts, the third line uses the definition of H^+ and the fourth line uses the fact that $\langle \hat{R}_\omega \cdot \mathbf{n}, \varphi \rangle = 0$, since φ is continuous and we consider the periodic boundary condition. In addition, we adopt (2.17), (6.1c) for the last line. Along the same line to obtain (6.4)–(6.5), we have

$$\begin{aligned}
 (R_q, \varphi) &= (\eta_q, \nabla \cdot \theta) - H^-(\eta_q, \Pi\theta) - (R_s, \Pi\theta - \theta) - (R_s, \theta), \\
 -(R_s, \theta) &= (\sigma - P\sigma, \nabla \cdot R_s) - \langle (R_s - \hat{R}_s) \cdot \mathbf{n}, \sigma - P\sigma \rangle.
 \end{aligned}$$

Thus we complete the proof by combining the above equalities. □

Now we are ready to prove the optimal error estimates of the elliptic projections. Take $z = PR_u$ in (6.3) and denote each line of the right hand in (6.3) by $\mathcal{S}_i, i = 1, 2, 3, 4$. Then the approximation properties (2.18)–(2.19) and the triangle inequality yield

$$\mathcal{S}_1 \leq Ch^{k+1}(\|\Pi\xi\| + \|\Pi\theta\|) \leq Ch^{k+1}(\|\xi\|_{H^1(\Omega)} + \|\theta\|_{H^3(\Omega)}).$$

By Cauchy–Schwarz inequality and (2.18), we derive

$$\begin{aligned}
 \mathcal{S}_2 &\leq C\|R_\omega\|h^{\min\{1, k+1\}}\|\xi\|_{H^1(\Omega)} + C\|R_q\|h^{\min\{2, k+1\}}\|\varphi\|_{H^2(\Omega)} \\
 &\quad + C\|R_s\|h^{\min\{3, k+1\}}\|\theta\|_{H^3(\Omega)} \\
 &\leq Ch(\|PR_u\| + h^{k+1})(\|\xi\|_{H^1(\Omega)} + \|\varphi\|_{H^2(\Omega)} + \|\theta\|_{H^3(\Omega)})
 \end{aligned}$$

for $k \geq 1$. Here we use the estimates in Lemma 6.1. It follows from the triangle inequality, the inverse inequality, the property (2.18) and Lemma 6.1 that

$$\begin{aligned} S_3 &\leq \|\varphi - P\varphi\|(\|\nabla \cdot \eta_\omega\| + \|\nabla \cdot \Pi R_\omega\|) + \|\sigma - P\sigma\|(\|\nabla \cdot \eta_s\| + \|\nabla \cdot \Pi R_s\|) \\ &\leq Ch^{\min\{1,k\}}\|\varphi\|_{H^2(\Omega)}(h^{k+1} + \|\Pi R_\omega\|) + Ch^{\min\{3,k\}}\|\sigma\|_{H^4(\Omega)}(h^{k+1} + \|\Pi R_s\|) \\ &\leq Ch(\|PR_u\| + h^{k+1})(\|\varphi\|_{H^2(\Omega)} + \|\sigma\|_{H^4(\Omega)}). \end{aligned}$$

For the last term S_4 , we adopt (2.18) and Lemma 6.1 to obtain

$$\begin{aligned} S_4 &\leq \|R_\omega \cdot \mathbf{n}\|_{\mathcal{E}_h}\|\varphi - P\varphi\|_{\mathcal{E}_h} + \|R_s \cdot \mathbf{n}\|_{\mathcal{E}_h}\|\sigma - P\sigma\|_{\mathcal{E}_h} \\ &\leq Ch^{\min\{1,k\}}\|\varphi\|_{H^2(\Omega)}(h^{k+1} + \|PR_u\|) + Ch^{\min\{3,k\}}\|\sigma\|_{H^4(\Omega)}h^{k+1} \\ &\leq Ch(\|PR_u\| + h^{k+1})(\|\varphi\|_{H^2(\Omega)} + \|\sigma\|_{H^4(\Omega)}). \end{aligned}$$

Adding the estimates of S_i , $i = 1, 2, 3, 4$ to the equality (6.3) and by the elliptic regularity (3.27), we have

$$\begin{aligned} \|PR_u\|^2 &\leq Ch(\|PR_u\| + h^{k+1})(\|\xi\|_{H^1(\Omega)} + \|\varphi\|_{H^2(\Omega)} + \|\theta\|_{H^3(\Omega)} + \|\sigma\|_{H^4(\Omega)}) \\ &\leq CC_*h(\|PR_u\| + h^{k+1})\|PR_u\|. \end{aligned}$$

Thus we can obtain the optimal error estimate (3.28) of the elliptic projection by the Young’s equality, the triangle inequality and Lemma 6.1.

References

1. Ciarlet, P.: The Finite Element Method for Elliptic Problem. North Holland, Amsterdam (1975)
2. Cockburn, B., Shu, C.-W.: The local discontinuous Galerkin method for time-dependent convection-diffusion systems. *SIAM J. Numer. Anal.* **35**, 2440–2463 (1998)
3. Cockburn, B., Shu, C.-W.: Runge–Kutta discontinuous Galerkin methods for convection-dominated problems. *J. Sci. Comput.* **16**, 173–261 (2001)
4. Cockburn, B., Kanschat, G., Perugia, I., Schötzau, D.: Superconvergence of the local discontinuous Galerkin method for elliptic problems on cartesian grids. *SIAM J. Numer. Anal.* **39**, 264–285 (2001)
5. Cross, M., Hohenberg, P.C.: Pattern formation outside of equilibrium. *Rev. Mod. Phys.* **65**, 851–1112 (1993)
6. Dutt, A., Greengard, L., Rokhlin, V.: Spectral deferred correction methods for ordinary differential equations. *BIT* **40**, 241–266 (2000)
7. Dong, B., Shu, C.-W.: Analysis of a local discontinuous Galerkin method for fourth-order time-dependent problems. *SIAM J. Numer. Anal.* **47**, 3240–3268 (2009)
8. Feng, X., Tang, T., Yang, J.: Long time numerical simulations for phase-field problems using p-adaptive spectral deferred correction methods. *SIAM J. Sci. Comput.* **37**, A271–A294 (2015)
9. Guo, R., Ji, L., Xu, Y.: High order local discontinuous Galerkin methods for the Allen-Cahn equation: analysis and simulation. *J. Comput. Math.* **34**, 135–158 (2016)
10. Guo, R., Xu, Y.: A high order adaptive time-stepping strategy and local discontinuous Galerkin method for the modified phase field crystal equation. *Commun. Comput. Phys.* **24**, 123–151 (2018)
11. Gong, Y., Zhao, J., Wang, Q.: Arbitrarily high-order unconditionally energy stable SAV schemes for gradient flow models. *Comput. Phys. Commun.* **249**, 107033 (2020)
12. Hutt, A., Atay, F.M.: Analysis of nonlocal neural fields for both general and gamma-distributed connectivities. *Phys. D Nonlinear Phenom.* **203**, 30–54 (2005)
13. Lee, H.G.: A semi-analytical Fourier spectral method for the Swift–Hohenberg equation. *Comput. Math. Appl.* **74**, 1885–1896 (2017)
14. Liu, H., Yin, P.: Unconditionally energy stable DG schemes for the Swift–Hohenberg equation. *J. Sci. Comput.* **81**, 789–819 (2019)
15. Liu, H., Yin, P.: High order unconditionally energy stable RKDG schemes for the Swift–Hohenberg equation. *J. Comput. Appl. Math.* **407**, 114015 (2022)
16. Minion, M.: Semi-implicit spectral deferred correction methods for ordinary differential equations. *Commun. Math. Sci.* **1**, 471–500 (2003)

17. Qi, L., Hou, Y.: A second order energy stable BDF numerical scheme for the Swift–Hohenberg equation. *J. Sci. Comput.* **88**, 1–25 (2021)
18. Reed, W., Hill, T.: Triangular mesh methods for the neutron transport equation. Technical report LA-UR-73-479. Los Alamos Scientific Laboratory, Los Alamos (1973)
19. Swift, J., Hohenberg, P.C.: Hydrodynamic fluctuations at the convective instability. *Phys. Rev. A* **15**, 319–328 (1977)
20. Swift, J., Hohenberg, P.C.: Effects of additive noise at the onset of Rayleigh–Benard convection. *Phys. Rev. A* **46**, 4773–4785 (1992)
21. Song, H., Shu, C.-W.: Unconditionally energy stability analysis of a second order implicit-explicit local discontinuous Galerkin method for the Cahn–Hilliard equation. *J. Sci. Comput.* **73**, 1178–1203 (2017)
22. Shen, J., Xu, J., Yang, J.: The scalar auxiliary variable (SAV) approach for gradient flows. *J. Comput. Phys.* **353**, 407–416 (2017)
23. Shen, J., Xu, J., Yang, J.: A new class of efficient and robust energy stable schemes for gradient flows. *SIAM Rev.* **61**, 474–506 (2019)
24. Tang, T., Xie, H., Yin, X.: High-order convergence of spectral deferred correction methods on general quadrature nodes. *J. Sci. Comput.* **56**, 1–13 (2012)
25. Wang, H., Zhang, Q., Shu, C.-W.: Stability analysis and error estimates of local discontinuous Galerkin methods with implicit-explicit time-marching for the time-dependent fourth order PDEs. *ESAIM Math. Model. Numer. Anal.* **51**, 1931–1955 (2017)
26. Xia, Y., Xu, Y., Shu, C.-W.: Efficient time discretization for local discontinuous Galerkin methods. *Discrete Contin. Dyn. Syst. Ser. A* **8**, 677–693 (2007)
27. Xu, Y., Shu, C.-W.: Local discontinuous Galerkin methods for high-order time-dependent partial differential equations. *Commun. Comput. Phys.* **7**, 1–46 (2010)
28. Xu, Y., Shu, C.-W.: Optimal error estimates of the semi-discrete local discontinuous Galerkin methods for high order wave equations. *SIAM J. Numer. Anal.* **50**, 79–104 (2012)
29. Zhang, Z., Ma, Y.: On a large time-stepping method for the Swift–Hohenberg equation. *Adv. Appl. Math. Mech.* **8**, 992–1003 (2016)

Publisher’s Note Springer Nature remains neutral with regard to jurisdictional claims in published maps and institutional affiliations.

Springer Nature or its licensor holds exclusive rights to this article under a publishing agreement with the author(s) or other rightsholder(s); author self-archiving of the accepted manuscript version of this article is solely governed by the terms of such publishing agreement and applicable law.